ANALYSIS OF A LOCAL DIFFUSIVE SIR MODEL WITH SEASONALITY AND NONLOCAL INCIDENCE OF INFECTION[*]

ZHUANZHUAN LIU[†], ZHONGWEI SHEN[‡], HAO WANG[§], AND ZHEN JIN[¶]

Abstract. For infectious diseases such as influenza and brucellosis, the susceptibility of a susceptible highly depends on the distance from each adjacent infectious individual. Such a propagation mechanism is often modeled by a nonlocal incidence with a kernel function $K(x)$, whose support determines the effective infection area. This nonlocal incidence of infection, together with important seasonal factors, leads to a periodic kernel function $K(t,x)$ and periodic parameters in a diffusive susceptible-infectious-recovered (SIR) model equipped with homogeneous Neumann boundary conditions. We first study the global well-posedness and the dissipativity of solutions. This is followed by the investigation of the global dynamics in terms of the basic reproduction number $\mathcal{R}_0$ defined to be the spectral radius of the next infection operator. The following results are shown rigorously: (1) If $\mathcal{R}_0 < 1$, the disease-free periodic solution is globally asymptotically stable. (2) If $\mathcal{R}_0 > 1$, the model is uniformly persistent and admits an endemic periodic solution. When the support size of $K(t,x)$ tends to 0, the basic reproduction number takes the $\mathcal{R}_0$ of the local infection model as the limit. Without seasonality, $\mathcal{R}_0$ and the endemic size of $I(t)$ (i.e., the total number of infected individuals at time t in the studied area) both decrease when the support size of $K(x)$ increases; however, there is no uniform result for the value and time of the disease outbreak peak. We also explore the integrated impact of seasonality and the infection rate β on $I(t)$. In addition, when the support size of $K(t,x)$ increases, the time difference between the first peak and the last peak of $I(t,x)$ decreases, and when the support size of $K(t,x)$ is large enough, the disease outbreak occurs almost simultaneously in the whole region. Moreover, due to seasonality not all locations experience a major disease outbreak in the early stage of disease transmission when the support size of $K(t,x)$ is relatively small.

Key words. diffusive SIR model, nonlocal incidence, seasonal effect, basic reproduction number, uniform persistence

AMS subject classifications. 37L45, 92D30, 45J05

DOI. 10.1137/18M1231493

1. Introduction. Infectious diseases are caused by infectious agents including viruses, bacteria, nematodes, and fungi that can be transmitted between humans, between animals, or between humans and animals. Not only does each large-scale outbreak of infectious disease threaten the life of humans by causing death or other diseases such as respiratory diseases and neurological diseases, but it also makes se-

[†]School of Data Science and Technology and School of Science, North University of China, Taiyuan, Shanxi 030051, PR China (liuzz428@163.com).

[‡]Department of Mathematical and Statistical Sciences, University of Alberta, Edmonton, AB T6G 2G1, Canada (zhongwei@ualberta.ca).

[§]Corresponding author. Department of Mathematical and Statistical Sciences, University of Alberta, Edmonton, AB T6G 2G1, Canada (hao8@ualberta.ca).

[¶]Complex Systems Research Center, Shanxi Key Laboratory of Mathematical Techniques and Big Data Analysis on Disease Control and Prevention, and Key Discipline of Computer Science and Technology of "Double-First-Class" Project of Shanxi Province, Shanxi University, Taiyuan, Shanxi 030006, PR China (jinzhn@263.net).

rious negative impacts on economics. In recent years, many diseases could be well controlled to cause fewer deaths due to great improvements in living environments and rapid progress in medical sciences. However, by virtue of the emergence of new viruses, the mutation of existing viruses, and the change of social behaviors, there are new challenges in controlling outbreaks of rapidly spreading infectious diseases such as SARS in 2003 and evolving existing diseases such as influenza. Therefore, it is of great significance to study the culprits, fundamental rules, and transmission mechanisms of infectious disease outbreaks for the sake of prevention and control. Mathematical models, especially differential equation models, have been proven to be a very important tool in understanding the underlying mechanisms of disease transmission and providing constructive control and preventive methods.

In 1927, the classical Kermack–McKendrick susceptible-infectious-recovered (SIR) compartment model was established when McKendrick and Kermack were studying the spread of the Black Death in London during 1665–1666 and the plague in Bombay during 1906 (see [13, 14, 15, 16]). In their model, McKendrick and Kermack included three mutually exclusive compartments: susceptibles (S), infected individuals (I), and recovered individuals (R), which become building blocks for almost all epidemic models. Introducing birth and death into the Kermack–McKendrick model, Hethcote established in [8] the following ordinary differential equation (ODE) model:

$$(1.1) \qquad \begin{cases} \dot{S} = b - \beta S I - \mu_1 S, \\ \dot{I} = \beta S I - \gamma I - \mu_2 I, \\ \dot{R} = \gamma I - \mu_3 R, \end{cases}$$

which becomes the Kermack–McKendrick model when the birth rate $b = 0$ and death rates $\mu_1 = \mu_2 = \mu_3 = 0$, where γ is the recovered rate and β is the infection rate. Since then, enormously many ODE models, including SI models, SIRS models, SIRI models, SEI models, and SEIR models, have been established to study the spread of infectious diseases. The mathematical analysis of these epidemic models mainly focuses on the global dynamics in terms of the basic reproduction number, which is defined to be the number of newly infected individuals that one infectious individual could produce during its infectious period in a population consisting of only susceptible individuals. In general, the disease becomes endemic when the basic reproduction number is greater than one. We refer the reader to [1, 4, 9, 24] and references therein for summaries and extensive remarks.

As we know, ODE models are relatively simple and easy to deal with, but they ignore spatial heterogeneity and movements of individuals, and of course cannot exhibit spatial patterns of the diseases. In addition, the outbreak predictions and the basic reproduction number can have severe departures from reality. To study the impact of spatial distribution and movements of individuals on the spread of diseases, Webb analyzed in [33] the classical Kermack–McKendrick model with diffusion and homogeneous Neumann boundary conditions on an interval. For partial differential equation (PDE) models, if we consider the factors including birth, death, migration, delay, spatio-temporal movements of individuals, infection age, spatial heterogeneity, and so on, the dynamical behaviors become much more complicated [2, 10, 19, 27, 34].

In the aforementioned PDE models, the transmission of diseases is assumed to occur by direct contact between susceptible and infectious individuals at the same location. However, some diseases can spread over long distances. For instance, an infected person with influenza can infect other persons in the same room, and animals with brucellosis can transmit the pathogen to susceptible animals through secretions,

excretions, and miscarriages. That is, the susceptible individuals may be infected by infectious individuals at different locations. To model such nonlocal contacts, de Mottoni, Orlandi, and Tesei studied in [23] the following system with nonlocal incidence of infection:

(1.2)
$$\begin{cases} S_t = \Delta S + b - dS - S \int_\Omega K(x-y)I(t,y)dy, & x \in \Omega, \\ I_t = \nu\Delta I + S \int_\Omega K(x-y)I(t,y)dy - \gamma I, & x \in \Omega, \\ \mathbf{n}(x) \cdot \nabla S(t,x) = \mathbf{n}(x) \cdot \nabla I(t,x) = 0, & x \in \partial\Omega, \end{cases}$$

where b, d, and γ are birth, death, and recovered rates, respectively, ν is the diffusion coefficient of infected individuals, and $\Omega \subset \mathbb{R}^N$ is a connected and bounded domain with smooth boundary. The function K is a compactly supported probability density function on $\mathbb{R}^N$, and $K(x-y)$ weights the contributions of the infected individuals at location y to the infection of susceptibles at location x. This gives rise to the nonlocal incidence of infection $S(x) \int_\Omega \beta K(x-y)I(y)dy$ at the location x. In [23], the authors studied the local and global asymptotic stability of the disease-free equilibrium $(\frac{b}{d}, 0)$ when $b < \frac{\gamma}{d}$. However, the basic reproduction number was not defined. Similar nonlocal incidence of infection was considered in [31], where the author investigated a class of SIR models with nonlocal incidence in infinite dimension and studied the global dynamics of solutions in terms of the basic reproduction number using a Lyapunov function whose construction was inspired by [6, 22].

In addition to spatial movements of individuals and nonlocal incidence of infection, seasonality and any other periodic change of environmental conditions are very important for many infectious diseases [3, 5, 29]. As shown in [5], influenza has a distinct seasonal nature in temperate regions. In [29], the authors pointed out that the infectious ability of the influenza virus is stronger in winter and spring in temperate regions. The prevalence of sheep brucellosis is also prominent. The sheep brucellosis usually begins in late winter and early spring, peaks in summer, and declines gradually in fall [28]. In consideration of these phenomena, we incorporate the periodicity into the nonlocal incidence and parameters. Under the assumption that recovered individuals have permanent immunity, we investigate the following model:

(1.3)
$$\begin{cases} S_t = \mu(t)\Delta S + \Lambda(t) - d(t)S - \beta S \int_\Omega K(t, x-y)I(t,y)dy, & x \in \Omega, \\ I_t = \nu(t)\Delta I - \kappa(t)I + \beta S \int_\Omega K(t, x-y)I(t,y)dy, & x \in \Omega, \\ \mathbf{n}(x) \cdot \nabla S(t,x) = \mathbf{n}(x) \cdot \nabla I(t,x) = 0, & x \in \partial\Omega, \end{cases}$$

where $\Omega \subset \mathbb{R}^N$ is a connected and bounded domain with smooth boundary, and the unknown functions $S(t,x)$ and $I(t,x)$ are the densities of susceptibles and infectives at location x and time t, respectively. The number $\beta > 0$ is the infection rate. $\mu(t)$ and $\nu(t)$ are diffusion coefficients of susceptibles and infectives at time t, respectively. $\Lambda(t)$ and $d(t)$ are the birth and death rates of susceptibles at time t, respectively. $\kappa(t)$ is the removal rate of infectives at time t. The functions $\mu(t)$, $\nu(t)$, $\Lambda(t)$, $d(t)$, and $\kappa(t)$ are continuous, positive, and T-periodic, where T typically equals 4 standing for the seasons. For each $x \in \mathbb{R}^N$, $t \mapsto K(t,x)$ is nonnegative, continuous, and T-periodic. For each $t \in \mathbb{R}$, $x \mapsto K(t,x)$ is a compactly supported probability density function on $\mathbb{R}^N$, and its support determines the effective infection area at time t. The kernel $K(t, x-y)$ weights the contributions of the infected individuals at location y to the infection of susceptibles at location x at time t, and it reflects the level of infection influence of an infective at location y on a susceptible at location x. The term $\beta S(t,x) \int_\Omega K(x-y)I(t,y)dy$ provides the nonlocal incidence at location x and time t.

This paper is organized as follows. In section 2, we study the global well-posedness and dissipativity of system (1.3). In section 3, we define the basic reproduction number of the system by the spectral radius of a next infection operator and determine the threshold dynamical behaviors. In section 4, we discuss the dependence of the basic reproduction number on the effective infection area of the nonlocality. In section 5, we provide numerical simulations to illustrate theoretical results and to exhibit some new observations. Finally, we give a brief discussion in section 6.

2. Global well-posedness and dissipativity. In this section, we study the global well-posedness and the global dissipativity of (1.3) with nonnegative initial data. For convenience, we set $\mathbb{R}_+ = [0, \infty)$ and define the following spaces: $C(\overline{\Omega}) = \{u : \overline{\Omega} \to \mathbb{R} : u \text{ is continuous}\}$, $C_+(\overline{\Omega}) = \{u \in C(\overline{\Omega}) : u \geq 0 \text{ on } \overline{\Omega}\}$, and $C_{++}(\overline{\Omega}) = \{u \in C(\overline{\Omega}) : u > 0 \text{ on } \overline{\Omega}\}$. The space $C(\overline{\Omega})$ is a Banach space equipped with the max norm $\|\cdot\|_\infty$.

We further set $X = C(\overline{\Omega}) \times C(\overline{\Omega})$, $X_+ = C_+(\overline{\Omega}) \times C_+(\overline{\Omega})$, and $X_{++} = C_{++}(\overline{\Omega}) \times C_{++}(\overline{\Omega})$. Then, X is a Banach space with norm $\|(u_1, u_2)\|_X := \|u_1\|_\infty + \|u_2\|_\infty$. Moreover, let $\mathcal{D} := \{v \in C(\overline{\Omega}) : \Delta v \in C(\overline{\Omega}) \text{ and } \mathbf{n} \cdot \nabla v = 0 \text{ on } \partial\Omega\}$.

The global well-posedness of (1.3) in X_+ is stated in the next result, whose proof is given in Appendix A.

THEOREM 2.1 (global well-posedness in X_+). *For any $(S_\tau, I_\tau) \in X_+$, (1.3) admits a unique classical solution $(S, I) \in C([\tau, \infty), X_+) \cap C^1((\tau, \infty), \mathcal{D} \times \mathcal{D})$ with initial data (S_τ, I_τ) at the initial moment τ. Moreover, if $(S_\tau, I_\tau) \in X_+$ and $I_\tau \not\equiv 0$, then $(S(t), I(t)) \in X_{++}$ for all $t \in (\tau, \infty)$.*

For $(S_\tau, I_\tau) \in X_+$, let $(S, I) \in C([\tau, \infty), X_+) \cap C^1((\tau, \infty), \mathcal{D} \times \mathcal{D})$ be the unique solution of (1.3) given in Theorem 2.1. The nonlinear evolution family $\{\Sigma(t, \tau)\}_{t \geq \tau}$ on X_+ generated by the solutions of (1.3) is defined as follows:

$$\Sigma(t, \tau)(S_\tau, I_\tau) = (S(t), I(t)), \quad t \geq \tau.$$

By the uniqueness of solutions of (1.3), there holds $\Sigma(t, \tau) = \Sigma(t, s)\Sigma(s, \tau)$ for $t \geq s \geq \tau$. By periodicity, there holds $\Sigma(t + T, \tau + T) = \Sigma(t, \tau)$ for $t \geq \tau$.

Let $\mathcal{P} := \Sigma(T, 0)$ be the time-T map (or the Poincaré map). The dissipativity of the dynamical system $(X_+, \{\mathcal{P}^n\}_{n \in \mathbb{N}_0})$ is stated in the next result, whose proof is given in Appendix A.

THEOREM 2.2. *The dynamical system $(X_+, \{\mathcal{P}^n\}_{n \in \mathbb{N}_0})$ admits a global attractor $\mathcal{A}$, that is, $\mathcal{A} \subset X_+$ is a compact invariant set of $\mathcal{P}$ and attracts bounded sets in the sense that for any bounded set $B \subset X_+$, there holds $\lim_{n \to \infty} d_H(\mathcal{P}^n B, \mathcal{A}) = 0$, where d_H denotes the Hausdorff semidistance.*

Theorem 2.2 immediately implies the global dissipativity of the nonlinear evolution family $\{\Sigma(t, \tau)\}_{t \geq \tau}$.

COROLLARY 2.1. *The evolution family $\{\Sigma(t, \tau)\}_{t \geq \tau}$ admits a periodic attractor $\{\mathcal{A}(t)\}_{t \in \mathbb{R}}$, that is, $\mathcal{A}(t) \subset X_+$ is compact for all $t \in \mathbb{R}$, $\mathcal{A}(t + T) = \mathcal{A}(t)$ for $t \in \mathbb{R}$, $\Sigma(t, \tau)\mathcal{A}(\tau) = \mathcal{A}(t)$ for $t \geq \tau$, and $\{\mathcal{A}(t)\}_{t \in \mathbb{R}}$ attracts bounded sets in the sense that for any bounded set $B \subset X_+$ and $\tau \in \mathbb{R}$ there holds $\lim_{t \to \infty} d_H(\Sigma(t, \tau)B, \mathcal{A}(t)) = 0$.*

We remark that Corollary 2.1 cannot tell whether the disease eventually becomes endemic or not, as the set $\cup_{t \in \mathbb{R}} (\{t\} \times \mathcal{A}(t))$ controlling the asymptotic dynamics in general contains both disease-free and endemic states. We investigate this issue in section 3.

3. Persistence theory. In this section, we first define the basic reproduction number and study its relation to the principal eigenvalue that determines the local stability of the disease-free periodic solution. Then, we investigate the global dynamics in terms of the basic reproduction number or the principal eigenvalue.

3.1. The basic reproduction number. In the absence of the disease, namely, $I \equiv 0$, the system (1.3) is reduced to $u_t = \Delta S + \Lambda(t) - d(t)S$ with homogeneous Neumann boundary condition, which is further reduced to

$$(3.1) \qquad \dot{S} = \Lambda(t) - d(t)S,$$

if we only consider spatially homogeneous solutions. The next result follows from standard arguments using the comparison principle and contracting arguments.

LEMMA 3.1. *The equation* (3.1) *admits a unique positive T-periodic solution, denoted by $S^0(t)$. Moreover, any solution $S(t, t_0)$ of* (3.1) *with a nonnegative initial datum at the initial moment $t_0 \in \mathbb{R}$ satisfies $\lim_{t \to \infty} |S(t, t_0) - S^0(t)| = 0$.*

DEFINITION 3.1. *We call $(S^0(t), 0)$ the* disease-free periodic solution *of the system* (1.3).

To study the dynamics of solutions, it is of great importance to know the local stability of the disease-free periodic solution $(S^0(t), 0)$. For this purpose, we consider the linearization of (1.3) at $(S^0(t), 0)$, namely,

$$\begin{cases} S_t = \mu(t)\Delta S - d(t)S - \beta S^0(t) \int_\Omega K(t, x - y)I(t, y)dy, & (t, x) \in \mathbb{R} \times \Omega, \\ I_t = \nu(t)\Delta I - \kappa(t)I + \beta S^0(t) \int_\Omega K(t, x - y)I(t, y)dy, & (t, x) \in \mathbb{R} \times \Omega, \\ \mathbf{n}(x) \cdot \nabla S(t, x) = \mathbf{n}(x) \cdot \nabla I(t, x) = 0, & (t, x) \in \mathbb{R} \times \partial\Omega. \end{cases}$$

Note that the I-equation only involves itself. Therefore, instead of considering the whole linearized system, it is more convenient to consider only the I-equation, that is,

$$(3.2) \quad \begin{cases} I_t = \nu(t)\Delta I - \kappa(t)I + \beta S^0(t) \int_\Omega K(t, x - y)I(t, y)dy, & (t, x) \in \mathbb{R} \times \Omega, \\ \mathbf{n}(x) \cdot \nabla I(t, x) = 0, & (t, x) \in \mathbb{R} \times \partial\Omega. \end{cases}$$

Associated with (3.2), we define two operators. We recall the definition of the evolution family $\{U_2(t, \tau)\}_{t \geq \tau}$ from Appendix A. Following [11, 20, 21, 27, 32, 35, 36], the first one is the *next infection operator* $\mathcal{N} : C_T(\mathbb{R} \times \overline{\Omega}) \to C_T(\mathbb{R} \times \overline{\Omega})$ defined as follows:

$$\mathcal{N}[\phi](t, x) = \beta \int_0^\infty U_2(t, t - s) \left[S^0(t - s) \int_\Omega K(t - s, \cdot - y)\phi(t - s, y)dy \right](x)ds$$

for $(t, x) \in \mathbb{R} \times \overline{\Omega}$ and $\phi \in C_T(\mathbb{R} \times \overline{\Omega})$, where

$$C_T(\mathbb{R} \times \overline{\Omega}) = \left\{ \phi \in C(\mathbb{R} \times \overline{\Omega}) : \phi(\cdot + T, \cdot) = \phi \right\}.$$

If ϕ is the initial distribution of infectious individuals, then $\beta S^0(t - s) \int_\Omega K(t - s, \cdot - y)\phi(t - s, y)dy$ is the distribution of newly infected individuals at time $t - s$, and $\beta U_2(t, t - s) \left[S^0(t - s) \int_\Omega K(t - s, \cdot - y)\phi(t - s, y)dy \right]$ is the distribution of infected individuals who were newly infected at time $t - s$ and remain infected at time t. Hence, $\mathcal{N}(t, \cdot)$ is the distribution of accumulative new infections at time t produced by all infectious individuals introduced before time t.

Remark 3.1. We make several remarks about the operator $\mathcal{N}$.

(1) We present a formal derivation of $\mathcal{N}$. Suppose $\phi \in C_T(\mathbb{R} \times \overline{\Omega})$ is an entire solution of (3.2). The variation of constants formula gives

$$\phi(t,x) = U_2(t,s)\phi(s,x) + \beta \int_s^t U_2(t,\tau)\left[S^0(\tau)\int_\Omega K(\tau, \cdot - y)\phi(\tau,y)dy\right](x)d\tau$$

for $(t,x) \in [s,\infty)\times\overline{\Omega}$. Setting $s \to -\infty$, the periodicity of ϕ and the properties of $U_2(t,s)$ ensure that $U_2(t,s)\phi(s,x) \to 0$ as $s \to -\infty$. Therefore,

$$\phi(t,x) = \beta \int_{-\infty}^t U_2(t,\tau)\left[S^0(\tau)\int_\Omega K(\tau, \cdot - y)\phi(\tau,y)dy\right](x)d\tau$$
$$= \beta \int_0^\infty U_2(t,t-s)\left[S^0(t-s)\int_\Omega K(t-s, \cdot - y)\phi(t-s,y)dy\right](x)ds$$

for $(t,x) \in \mathbb{R} \times \overline{\Omega}$. This suggests defining the operator $\mathcal{N}$ and implies that the spectral radius of $\mathcal{N}$ being 1 is a critical number.

(2) In the case of t-independent coefficients, looking for stationary solutions of (3.2) would suggest defining $\mathcal{N}$ as follows:

$$\mathcal{N}[\phi](x) = \beta S^0 \int_0^\infty e^{(\nu\Delta - \kappa id_{C(\overline{\Omega})})s}\left[\int_\Omega K(\cdot - y)\phi(y)dy\right](x)ds$$
$$= \beta S^0 \left(\kappa id_{C(\overline{\Omega})} - \nu\Delta\right)^{-1}\left[\int_\Omega K(\cdot - y)\phi(y)dy\right](x) \quad \forall x \in \overline{\Omega},$$

for $\phi \in C(\overline{\Omega})$, where Δ is equipped with the homogeneous Neumann boundary condition. We present an alternative derivation of $\mathcal{N}$ in this case. Clearly, (3.2) suggests considering the linear operator $\widetilde{\mathcal{N}} := \nu\Delta - \kappa id_{C(\overline{\Omega})} + F$, where $F : C(\overline{\Omega}) \to C(\overline{\Omega})$ is defined by $F[\phi] = \beta S^0 \int_\Omega K(\cdot - y)\phi(y)dy$. Then, the invertibility of the operator $\kappa id_{C(\overline{\Omega})} - \nu\Delta$ allows us to rewrite $\widetilde{\mathcal{N}}$ as

$$\widetilde{\mathcal{N}} = (\kappa id_{C(\overline{\Omega})} - \nu\Delta)\left[-id_{C(\overline{\Omega})} + (\kappa id_{C(\overline{\Omega})} - \nu\Delta)^{-1}F\right],$$

giving rise to the operator $(\kappa id_{C(\overline{\Omega})} - \nu\Delta)^{-1}F$, which is nothing but $\mathcal{N}$. Note that we can also rewrite $\tilde{\mathcal{N}}$ as

$$\widetilde{\mathcal{N}} = \left[-id_{C(\overline{\Omega})} + F(\kappa id_{C(\overline{\Omega})} - \nu\Delta)^{-1}\right](\kappa id_{C(\overline{\Omega})} - \nu\Delta).$$

This suggests considering the operator $F(\kappa id_{C(\overline{\Omega})} - \nu\Delta)^{-1}$, whose spectral radius has been frequently used to define the basic reproduction number in the literature, especially for corresponding SIR ODE models.

(3) If $\eta \neq 0$ and $\phi \in C_T(\mathbb{R} \times \overline{\Omega}) \setminus \{0\}$ satisfy $\mathcal{N}[\phi] = \eta\phi$, then $\phi \in \mathcal{D}_T(\mathbb{R} \times \overline{\Omega})$, due to the smoothing effects of the evolution family $\{U_2(t,\tau)\}_{t\geq\tau}$, and (η,ϕ) solves

$$(3.3) \quad \begin{cases} \phi_t = \nu(t)\Delta\phi - \kappa(t)\phi + \frac{\beta S^0(t)}{\eta}\int_\Omega K(t,x-y)\phi(t,y)dy, & x \in \Omega, \\ \mathbf{n}(x)\cdot\nabla\phi(t,x) = 0, & x \in \partial\Omega. \end{cases}$$

It is not hard to show that $\mathcal{N}$ is compact and strongly positive. By the Kreĭn–Rutman theorem (see, e.g., [18, 30]), the spectral radius $r(\mathcal{N})$ of $\mathcal{N}$ is an algebraically simple and isolated eigenvalue of $\mathcal{N}$ admitting a positive eigenfunction. Moreover, $r(\mathcal{N})$ is the only eigenvalue of $\mathcal{N}$ admitting a positive eigenfunction.

DEFINITION 3.2. *The number $\mathcal{R}_0 := r(\mathcal{N})$ is called the* basic reproduction number *of the system* (1.3).

Remark 3.2. We acknowledge that the definition of the basic reproduction number $\mathcal{R}_0$ in Definition 3.2 falls into the abstract framework established in [20], where the authors define the basic reproduction number, which is called the basic reproduction ratio in [20], for a large class of periodic abstract functional differential equations. Moreover, it is easy to check that the assumptions (H1), (H2), and (H6) in [20] are satisfied. As $\mathcal{R}_0 > 0$ (due to the compactness and strong positivity of $\mathcal{N}$), [20, Proposition 3.9] says that the assumptions (H3), (H4), and (H5) in [20] are also satisfied.

The second operator is $\mathcal{L} : \mathcal{D}_T(\mathbb{R} \times \overline{\Omega}) \to C_T(\mathbb{R} \times \overline{\Omega})$ defined by

$$\mathcal{L}[\phi](t,x) = -\phi_t(t,x) + \nu(t)\Delta\phi(t,x) - \kappa(t)\phi(t,x) + \beta S^0(t) \int_\Omega K(t, x-y)\phi(t,y) dy$$

for $(t,x) \in \mathbb{R} \times \overline{\Omega}$ and $\phi \in \mathcal{D}_T(\mathbb{R} \times \overline{\Omega})$, where

$$\mathcal{D}_T(\mathbb{R} \times \overline{\Omega}) = \left\{ \phi \in C_T(\mathbb{R} \times \overline{\Omega}) : \phi_t, \Delta\phi \in C_T(\mathbb{R} \times \overline{\Omega}), \mathbf{n} \cdot \nabla\phi = 0 \text{ on } \mathbb{R} \times \partial\Omega \right\}.$$

It is well known that $\mathcal{L}$ is resolvent compact, and therefore, the spectrum $\sigma(\mathcal{L})$ consists of isolated eigenvalues. The following result is classical (see, e.g., [7]).

LEMMA 3.2. *The operator $\mathcal{L}$ admits an eigenvalue λ_p with a positive eigenfunction ϕ_p, namely, $\phi_p \in \mathcal{D}_T(\mathbb{R} \times \overline{\Omega})$ satisfies $\phi_p(t,x) > 0$ for all $(t,x) \in \mathbb{R} \times \overline{\Omega}$ and the eigenequation $\mathcal{L}\phi_p = \lambda_p\phi_p$. Moreover, λ_p is algebraically simple and isolated. In addition, any $\lambda \in \sigma(\mathcal{L})\backslash\{\lambda_p\}$ satisfies $\Re\lambda < \lambda_p$ and admits only sign-changing eigenfunctions.*

The number λ_p given in the above lemma is often referred to as the *principal eigenvalue* of $\mathcal{L}$. It determines the local stability of the disease-free periodic solution. For each $c > 0$, $c\phi_p$ is called a *principal eigenfunction* of $\mathcal{L}$.

To connect $\mathcal{R}_0$ with λ_p, we consider the problem (3.3) for (η, ϕ) and prove the following result.

LEMMA 3.3. *The following statements hold.*
(1) *There is a unique $\eta > 0$, denoted by η_0, such that the problem* (3.3) *with $\eta = \eta_0$ admits a positive solution in $\mathcal{D}_T(\mathbb{R} \times \overline{\Omega})$. Moreover, $\mathcal{R}_0 = \eta_0$.*
(2) *$\eta_0 - 1$, and hence $\mathcal{R}_0 - 1$, has the same sign as λ_p.*

Proof. (1) By Remark 3.2, we can apply [20, Theorem 3.8] to draw the conclusion. Below, we give a short proof. On one hand, let $\phi \in C_T(\mathbb{R} \times \overline{\Omega})$ be positive and satisfy $\mathcal{N}\phi = \mathcal{R}_0\phi$. Then, Remark 3.1(3) says that $(\mathcal{R}_0, \phi)$ solves the problem (3.3).

On the other hand, if both (η_1, ϕ_1) and (η_2, ϕ_2) solve the problem (3.3) and ϕ_1 and ϕ_2 are positive, then Remark 3.1(2) ensures that $\mathcal{N}\phi_i = \eta_i\phi_i$ for $i = 1, 2$. That is, both η_1 and η_2 are eigenvalues of $\mathcal{N}$ with a positive eigenfunction. It then follows that $\eta_1 = \eta_2 = \mathcal{R}_0$.

(2) We refer the reader to the proof of [27, Lemma 2.2], where a similar problem is treated. By Remark 3.2, it is also a straightforward consequence of [20, Theorem 3.7]. $\square$

3.2. Threshold dynamics. Let $(S(t), I(t)) = (S(t, \cdot), I(t, \cdot))$ be the unique solution of (1.3) given in Theorem 2.1 with initial data (S_0, I_0) at the initial moment zero.

DEFINITION 3.3. *The system* (1.3) *is called* uniformly persistent *if there exists* $\epsilon_0 > 0$ *such that for any* $(S_0, I_0) \in X_+$ *with* $I_0 \not\equiv 0$, *there hold*

$$\liminf_{t \to \infty} \min_{x \in \overline{\Omega}} S(t, x) \geq \epsilon_0 \quad and \quad \liminf_{t \to \infty} \min_{x \in \overline{\Omega}} I(t, x) \geq \epsilon_0.$$

The result on the threshold dynamics is stated in the next result, whose proof is given in Appendix B.

THEOREM 3.1. *The following statements hold.*
(1) *If* $\mathcal{R}_0 < 1$, *then* $\lim_{t \to \infty} \left\| (S(t), I(t)) - (S^0(t), 0) \right\|_X = 0$ *for any* $(S_0, I_0) \in X_+$.
(2) *If* $\mathcal{R}_0 > 1$, *then the system* (1.3) *is uniformly persistent and admits a T-periodic solution lying in* X_{++}.

Theorem 3.1 shows that the disease eventually gets eradicated when $\mathcal{R}_0 < 1$, while it becomes endemic when $\mathcal{R}_0 > 1$. Moreover, endemic states exist when $\mathcal{R}_0 > 1$.

This leaves an interesting open problem—to study the uniqueness and the global asymptotic stability of the T-periodic solution in the case $\mathcal{R}_0 > 1$.

4. Effects of nonlocality. We study the effects of nonlocality on the basic reproduction number. For $a > 0$, let $K_a(t, x) = \frac{1}{a^N} K(t, \frac{x}{a})$ for $(t, x) \in \mathbb{R} \times \mathbb{R}^N$. When a decreases, the support size of $K_a(t, x)$ decreases, which means that the effective infection area decreases. We consider (1.3) with K replaced by K_a. The associated next infection operator reads

$$\mathcal{N}^a[\phi](t, x) = \beta \int_0^\infty U_2(t, t - s) \left[S^0(t - s) \int_\Omega K_a(t - s, \cdot - y)\phi(t - s, y)dy \right](x)ds$$

for $(t, x) \in \mathbb{R} \times \overline{\Omega}$ and $\phi \in C_T(\mathbb{R} \times \overline{\Omega})$. Denote by $\mathcal{R}_0^a = r(\mathcal{N}^a)$ the associated basic reproduction number.

Note that $K_a(t, \cdot)$ converges to δ_0 as $a \to 0^+$ for all $t \in \mathbb{R}$, where δ_0 is the Dirac function at 0. In this limiting case, the associated next infection operator reads

$$\mathcal{N}^0[\phi](t, x) = \beta \int_0^\infty U_2(t, t - s) \left[S^0(t - s)\phi(t - s, \cdot) \right](x)ds \quad \forall (t, x) \in \mathbb{R} \times \overline{\Omega}.$$

Denote by $\mathcal{R}_0^0 = r(\mathcal{N}^0)$ the associated basic reproduction number.

To study the effects of nonlocal incidence, we compare $\mathcal{R}_0^a$ with $\mathcal{R}_0^0$ and establish the following result, whose proof is presented in Appendix C.

THEOREM 4.1. *The following statements hold.*
(1) *There holds the limit* $\lim_{a \to 0^+} \mathcal{R}_0^a = \mathcal{R}_0^0$.
(2) *If* $\frac{\Lambda(t)}{d(t)}$ *and* $\kappa(t) = \kappa$ *are independent of* t, *then* $\mathcal{R}_0^a < \mathcal{R}_0^0$ *for each* $a > 0$.

In case (2) of Theorem 4.1, we prove that the basic reproduction number in the case of nonlocal incidence is smaller than that in the case of classical/local incidence, and hence, the disease in the case of nonlocal incidence is less likely to become endemic than that in the case of classical incidence. The reason causing this can be understood as follows: The infection rate β describes the intensity of the disease transmission. The nonlocal incidence describes the situation in which susceptible individuals at a location can be infected by infected individuals at other locations following a probability distribution, and nonlocal incidence reduces the intensity of disease transmission. Thus, the basic reproduction number is smaller in comparison to the local incidence.

5. Numerical simulations. In this section, we present numerical simulations based on sheep's brucellosis. Assuming that infected sheep are removed after death, we divide the sheep into three compartments: susceptible sheep (S), infected sheep (I), and removed sheep (R). Infected sheep can transmit brucellosis to susceptible sheep through secretions, excretions, and miscarriages. In particular, susceptible sheep can be infected by infected sheep in different locations. We use the kernel $K(t, x - y)$ to characterize the contribution of infected sheep at location y to the infection of susceptibles at location x. Therefore, the incidence at time t and location x is given by the nonlocal incidence term as in (1.3). For convenience, we assume that the activity range of sheep is $[0, l] \subset \mathbb{R}$, where $l > 0$, and the flux of sheep at each boundary is zero. Thus, we consider the following brucellosis model with homogeneous Neumann boundary conditions:

$$(5.1) \quad \begin{cases} S_t = \mu(t)S_{xx} + \Lambda(t) - d(t)S - \beta S \int_0^l K(t, x - y)I(t, y)dy, & x \in (0, l), \\ I_t = \nu(t)I_{xx} - \kappa(t)I + \beta S \int_0^l K(t, x - y)I(t, y)dy, & x \in (0, l), \\ S_x(t, 0) = S_x(t, l) = I_x(t, 0) = I_x(t, l) = 0, \end{cases}$$

where $\kappa(t)$ is the death rate of infected sheep (assuming no recovery), and the other parameters have the same meanings as those in (1.3).

As, in general, the contribution of the infected sheep to the infection of susceptibles becomes larger when the distance between them decreases, we use the following kernel function (5.2) (see the derivation of (5.2) in Remark 5.1):

$$(5.2) \quad K(t, x) = \begin{cases} \frac{1}{2a} \frac{1}{\mathrm{erfc}\left(\sqrt{\frac{1}{2\sigma(t)^2}}\right)} e^{-\frac{\sec^2(\frac{\pi}{2a}x)}{2\sigma(t)^2}}, & |x| < a, \quad t \in \mathbb{R}, \\ 0, & |x| \geq a, \quad t \in \mathbb{R}, \end{cases}$$

where $\mathrm{erfc}(x) = \frac{2}{\sqrt{\pi}} \int_x^\infty e^{-s^2} ds$ is the complementary error function, $\sigma(t)$ is a continuous and positive 4-periodic function, and $a > 0$ is a constant. It is easy to verify that for any $\sigma(t)$ and any $a > 0$, $\int_{-a}^a K(t, x)dx = 1$ for all $t \in \mathbb{R}$, and $K(t+4, x) = K(t, x)$ and $K(t, -x) = K(t, x)$ for all $(t, x) \in \mathbb{R} \times \mathbb{R}$. As the support of $x \mapsto K(t, x)$ is $[-a, a]$ for any $t \in \mathbb{R}$, the effective infection range of the infected sheep at location x is $[x - a, x + a]$. We call a the *effective infection radius.* In Figure 1(a), we plot $K(t, x)$ in two periods for $a = 1$ and $\sigma(t) = 3 + 2\sin(\frac{\pi}{2}t + \frac{\pi}{2})$.

(a) The kernel function $K(t, x)$.   (b) $\mathcal{R}_0$ versus β.
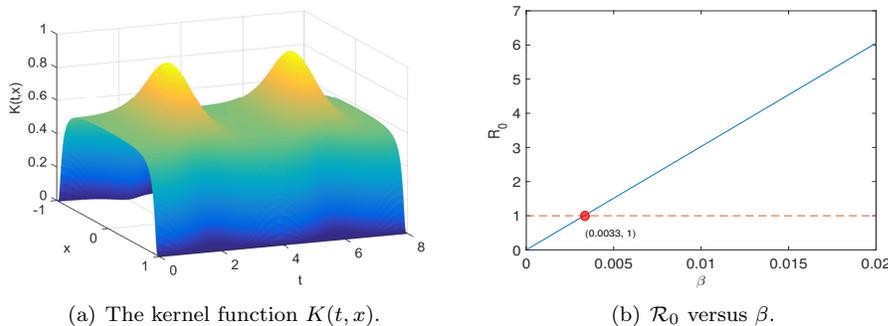
FIG. 1. *Graphs of the kernel function and the basic reproduction number.*

Remark 5.1. Changing variables $x \to \tan(\frac{\pi}{2a}x)$ in the Gaussian function $x \mapsto \frac{1}{\sqrt{2\pi}\sigma}e^{-\frac{x^2}{2\sigma^2}}$, we obtain the function $x \mapsto \frac{1}{\sqrt{2\pi}\sigma}e^{-\frac{\tan(\frac{\pi}{2a}x)^2}{2\sigma^2}}$ for $x \in (-a,a)$. For a positive 4-periodic function $\sigma(t)$, we define $K(t,x) = \frac{1}{A}\frac{1}{\sqrt{2\pi}\sigma(t)}e^{-\frac{\tan(\frac{\pi}{2a}x)^2}{2\sigma(t)^2}}$ for $x \in (-a,a)$ and $t \in \mathbb{R}$, where $A = \frac{1}{\sqrt{2\pi}\sigma(t)}\int_{-a}^{a}e^{-\frac{\tan(\frac{\pi}{2a}x)^2}{2\sigma(t)^2}}\,dx$ is such that $\int_{-a}^{a}K(t,x)dx = 1$ for all $t \in \mathbb{R}$. As $\int_{-\infty}^{\infty}\frac{e^{-\frac{x^2}{2B^2}}}{1+x^2}dx = \pi e^{\frac{1}{2B^2}}\mathrm{erfc}\big(\sqrt{\frac{1}{2B^2}}\big)$ for $Re(B^2) > 0$ (see, e.g., [25, item 7 on page 4]), we obtain $A = \frac{2a}{\sqrt{2\pi}\sigma(t)}e^{\frac{1}{2\sigma(t)^2}}\mathrm{erfc}\big(\sqrt{\frac{1}{2\sigma(t)^2}}\big)$.

5.1. The basic reproduction number. In this subsection, we introduce the theory of calculating $\mathcal{R}_0$ and provide the simulations of $\mathcal{R}_0$ and the asymptotic behaviors of (5.1). To do so, we consider the basic reproduction number $\mathcal{R}_0$ associated to the following equation:

$$\begin{cases} I_t = \nu(t)I_{xx} - \kappa(t)I + \beta S^0(t)\int_0^l K(t,x-y)I(t,y)dy, & x \in (0,l), \\ I_x(t,0) = 0 = I_x(t,l). \end{cases}$$

According to [20, Theorem 3.8], there holds $\mathcal{R}_0 = \frac{1}{\lambda_0}$, where λ_0 is the unique solution of the algebraic equation $r(U(4,0,\lambda)) = 1$. Here, $\{U(t,s,\lambda) : t \geq s\}$ is the evolution family of bounded linear operators on $C([0,l])$ generated by the following 4-periodic linear equation with parameter $\lambda \in [0,\infty)$:

$$\frac{du}{dt} = \lambda F(t)u(t) - V(t)u(t),$$

and $r(U(t,s,\lambda))$ is the spectral radius of the operator $U(t,s,\lambda)$, where for each $t \in \mathbb{R}$

$$V(t)\phi := -\nu(t)\phi_{xx} + \kappa(t)\phi,$$
$$F(t)\phi := \beta S^0(t)\int_\Omega K(t,\cdot - y)\phi(y)dy.$$

For each $\lambda \in [0,\infty)$, $r(U(4,0,\lambda))$ can be numerically computed according to [20, Lemma 2.5].

We take the effective infectious radius $a = 1$ km and $l = 50$ km. As brucellosis is more infectious in spring and summer, we take $\sigma(t) = 3 + 2\sin(\frac{\pi}{2}t + \frac{\pi}{2})$ and then choose $K(t,x)$ as in Figure 1(a). In China, sheep are mainly born from February to April and are slaughtered from October to December every year, and thus we choose $\Lambda(t) = 170 + 160\sin(\frac{\pi}{2}t)$, $d(t) = 0.17 + 0.15\sin(\frac{\pi}{2}t + \pi)$, and $\kappa(t) = 3.17 + 0.15\sin(\frac{\pi}{2}t + \pi)$. Taking into account that sheep are more active in spring and summer, we choose $\mu(t) = 10 + 4.5\sin(\frac{\pi}{2}t + 1.75\pi)$ and $\nu(t) = 5 + 2\sin(\frac{\pi}{2}t + 1.75\pi)$. The initial density $S_0(x)$ of susceptible sheep is

$$S_0(x) = 2252.3e^{\frac{25^2}{(x-25)^2 - 25^2}}, \quad |x - 25| \leq 25.$$

Suppose that the infected sheep concentrate in the interval $[24, 26]$ at the initial time, and the initial density $I_0(x)$ is

$$I_0(x) = \begin{cases} 22.523e^{\frac{1}{(x-25)^2 - 1}}, & |x - 25| \leq 1, \\ 0 & \text{otherwise.} \end{cases}$$

In Figure 1(b), we plot $\mathcal{R}_0$ with respect to β using the aforementioned method. It can be seen that $\mathcal{R}_0$ is a linear increasing function of β, and $\mathcal{R}_0 \approx 1$ when $\beta \approx 0.0033$.

(a) When $\beta = 0.003$, $\mathcal{R}_0 = 0.9038 < 1$. In this case, as time goes to infinity, the density of infected sheep converges to zero (see Figure 2(a)), and the density of susceptibles converges to a positive periodic function which is independent of x (see Figure 2(b)). This is compatible with the global asymptotic stability of the disease-free periodic solution proven in Theorem 3.1(1) when $\mathcal{R}_0 < 1$.

(b) When $\beta = 0.004$, $\mathcal{R}_0 = 1.2111 > 1$. In this case, Figures 3(a) and 3(c) show that both $I(t,x)$ and $S(t,x)$ converge to positive periodic functions. This is consistent with Theorem 3.1(2) stating that the system (5.1) is uniformly persistent and admits a positive 4-periodic solution when $\mathcal{R}_0 > 1$. In this case, we also sketch $I(t) = \int_0^l I(t,x)dx$ in a period in Figure 3(b) for $I(t,x)$ being the I-component of the positive periodic solution. It can be seen that sheep brucellosis peaks in summer and declines gradually in fall, which is basically in line with the actual situation.

These results show that when $\mathcal{R}_0 < 1$, sheep brucellosis disappears finally, but when $\mathcal{R}_0 > 1$, it eventually shows a certain seasonality, and the densities of susceptible and infected sheep have spatial heterogeneity. Furthermore, these results suggest that to control the spread of brucellosis, it is effective to reduce the contact rate of infected sheep with susceptibles.

(a) Spatio-temporal solution of $I(t,x)$.

(b) Spatio-temporal solution of $S(t,x)$.
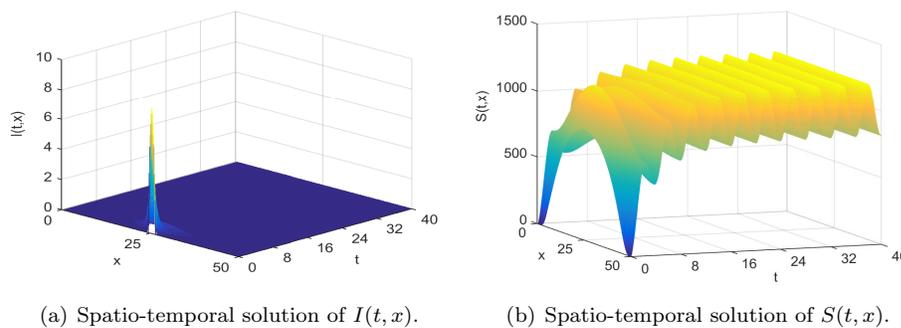
Fig. 2. *Simulation of the disease-free periodic solution when $\beta = 0.003$ ($\mathcal{R}_0 = 0.9531 < 1$).*

5.2. Significance of nonlocality. In this subsection, we provide numerical illustrations for Theorem 4.1 and investigate the effects of the effective infection radius a on the outbreak peak (the transient highest peak) and the endemic size of the disease. We mainly investigate the effects of nonlocality, and then we assume that all coefficients are independent of time. Choose $l = 50$, $\mu(t) = 10$, $\nu(t) = 5$, $d(t) = 0.17$, $\kappa(t) = 3.17$, $\Lambda(t) = 170$, $\beta = 0.00318$, and the kernel function as follows:

$$(5.3) \qquad K(x) = \begin{cases} \frac{2.2523}{a} e^{\frac{a^2}{x^2 - a^2}}, & |x| \le a, \\ 0, & |x| > a. \end{cases}$$

For example, we plot $K(x)$ with $a = 1$ in Figure 4(a). It is easy to verify that $\int_{-a}^{a} K(x)dx = 1$. Obviously, a is the effective infection radius. Let $a \to 0^+$; we obtain

(a) Spatio-temporal dynamics of $I(t,x)$.

(b) The steady solution in a period of $I(t)$.

(c) Spatio-temporal dynamics of $S(t,x)$.
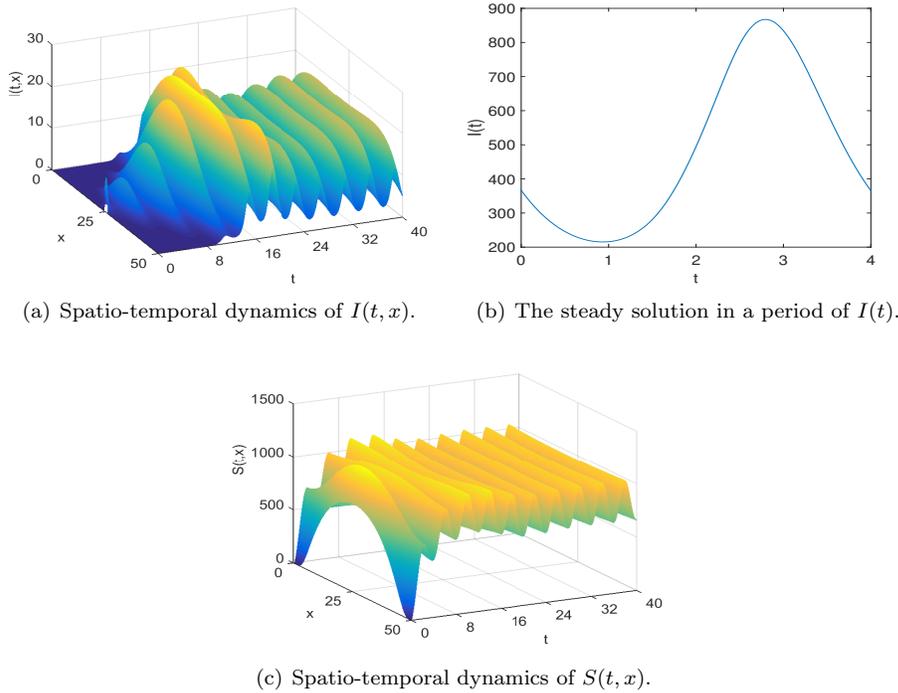
FIG. 3. *Simulation of the positive periodic solution when $\beta = 0.004$ ($\mathcal{R}_0 = 1.2684 > 1$).*

the local incidence model:

$$(5.4) \quad \begin{cases} S_t = \mu S_{xx} + \Lambda - dS - \beta SI, & x \in (0,l), \\ I_t = \nu I_{xx} - \kappa I + \beta SI, & x \in (0,l), \\ S_x(t,0) = S_x(t,l) = I_x(t,0) = I_x(t,l) = 0. \end{cases}$$

Denote $\mathcal{R}_0^a$ and $\mathcal{R}_0^0$ for the basic reproduction numbers of (5.1) and (5.4), respectively.

For the local system (5.4), according to the proof of Theorem 4.1, we obtain $\mathcal{R}_0^0 = \frac{\Lambda\beta}{\kappa d} = 1.003$ corresponding to the red point $(0, 1.003)$ in Figure 4(b). For the nonlocal system (5.1), the blue curve in Figure 4(b) shows that $\mathcal{R}_0^a$ is a decreasing function of a, and $\mathcal{R}_0^a \to \mathcal{R}_0^0 = 1.003$ as $a \to 0^+$. (Color available online.) Now we have provided numerical illustrations for Theorem 4.1 under the condition that all parameters are independent of time. The results seem counterintuitive. We believe that the increase of effective infection range causes more sheep to be infected, and thereby $\mathcal{R}_0$ increases. Indeed, without the consideration of cross-distance infected individuals, both β and $\mathcal{R}_0$ certainly decrease. However, the average infection rates are all β for any $a \geq 0$ in our model because the kernel function satisfies the normalization. What we want to discuss is how the basic reproduction number changes when the effective infection radius a becomes larger in the condition that the average infection rate remains unchanged. Note that the nonlocal incidence describes the situation in which susceptibles at a location can be infected by infected individuals at other locations following a probability distribution. Nonlocal incidence dilutes the intensity of β; moreover, the larger effective infection radius leads to the more severe dilution for β. It is precisely because of the dilution that $\mathcal{R}_0$ decreases. We can understand it

in this way: the infection rate is analogous to a force acting on a bar, and a force on the whole bar will not break the bar, but it is easy to break the bar when the same force concentrates on a point or smaller area on the bar. As a conclusion, in the case when the infection rate stays the same, the classical model with local infection can overestimate the outbreak of the disease.

(a) The spatial kernel function $K(x)$.   (b) $\mathcal{R}_0$: Local versus nonlocal.
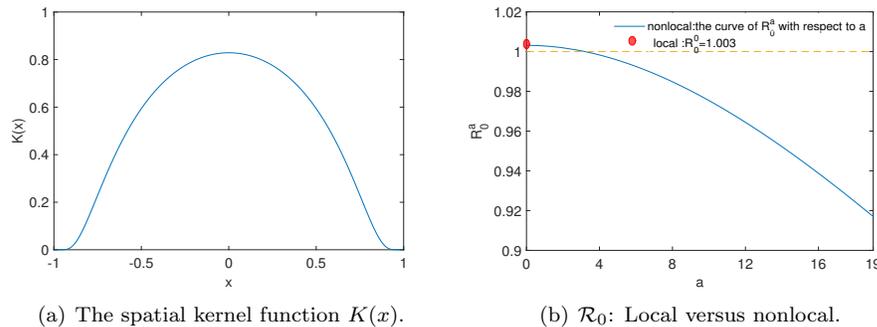
FIG. 4. *Graphs to illustrate the significance of nonlocality.*

Now, we investigate the effects of the effective infection radius a on the outbreak peak and the endemic size of the disease. Keep the initial conditions and the parameters unchanged except β and a. In general, $a < l/2$. The different values that we choose for β and a are listed as follows: $a = 0$ (i.e., local), $a = 5$, $a = 10$, $a = 20$, $a = 24$; $\beta = 0.004$, $\beta = 0.01$, $\beta = 0.1$. For each β, we draw the curves of $I(t)$, as shown in Figure 5. For the case of $\beta = 0.1$, we sketch the solution curves of $I(t)$ within nine seasons in Figure 5(c) and the steady states in Figure 5(d). Figure 5 shows that with the increase of a, the rate of change of $I(t)$ initially decreases gradually, which is consistent with the variation of $\mathcal{R}_0$. However, the variation ratio at the beginning does not determine the subsequent change. As we can see from Figure 5, when $\beta = 0.004$, the peak value decreases, and the peak time arrives later with the increase of a; when $\beta = 0.01$, the peak time arrives later, and the peak value first increases and then decreases; when $\beta = 0.1$, the situation is more complex. These phenomena show that the effective infection radius a has no uniform effects on the disease outbreak. However, Figure 5 illustrates that the increase of a leads to a smaller endemic size, which is consistent with ODE SIR models' conclusion that a larger $\mathcal{R}_0$ results in a smaller endemic size.

5.3. Significance of seasonality. In this subsection, in order to investigate the influence of seasonality, we compare the periodic system (5.1) (P.S.) with the corresponding time-averaged system (T.A.S.), namely,

$$(5.5) \quad \begin{cases} S_t = \overline{\mu} S_{xx} + \overline{\Lambda} - \overline{d} S - \beta S \int_0^l \overline{K}(x-y) I(t,y) dy, & x \in (0,l), \\ I_t = \overline{\nu} I_{xx} - \overline{\kappa} I + \beta S \int_0^l \overline{K}(x-y) I(t,y) dy, & x \in (0,l), \\ S_x(t,0) = S_x(t,l) = I_x(t,0) = I_x(t,l) = 0, \end{cases}$$

where $\overline{\mu}, \overline{\Lambda}, \overline{d}, \overline{\nu}, \overline{\kappa}$, and $\overline{K}$ are time averages of $\mu(t), \Lambda(t), d(t), \nu(t), \kappa(t)$, and $K(t,\cdot)$. More precisely, $\overline{\mu} = \frac{1}{4} \int_0^4 \mu(t) dt$, and the others are defined similarly. Let Q denote the studied quantity, and let Q(P.S.) and Q(T.A.S.) denote Q in the periodic system (5.1) and in the corresponding time-averaged system (5.5), respectively. Compared with

(a) The impact of a when $\beta = 0.004$.

(b) The impact of a when $\beta = 0.01$.

(c) The impact of a on the first disease outbreak when $\beta = 0.1$.

(d) The impact of a on the endemic size when $\beta = 0.1$.
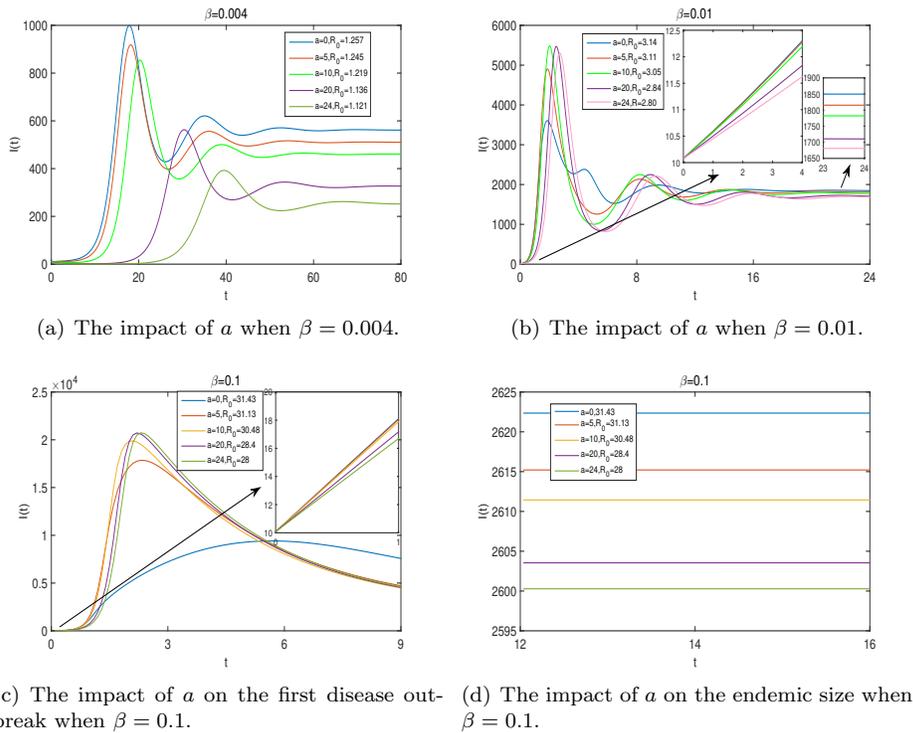
Fig. 5. *The impact of the effective infection radius a on the number of infectives $I(t)$.*

the periodic system, the change degree of Q (CD(Q)) in the time-averaged system is defined as

$$\mathrm{CD(Q)} = \frac{Q(\mathrm{T.A.S.}) - Q(\mathrm{P.S.})}{Q(\mathrm{P.S.})}.$$

Here Q's are cumulative numbers of infectives in one limiting period ($\lim\limits_{t \to \infty} \int_t^{t+4} I(t)dt$) (CNI), the magnitude of outbreak peak (MP), and the time of outbreak peak (TP). The parameters except β and initial conditions are the same as those in subsection 5.1. We plot the curves of CD(CNI), CD(MP), and CD(TP) with respect to $\beta \in [0.0033, 0.03]$, as shown in Figure 6(a). Note that we take $\beta \geq 0.0033$ in order to ensure $\mathcal{R}_0 > 1$, and the outbreak peak is the transient highest peak.

(a) The diagram of CD.

(b) Outbreak peak in P.S.

(c) Outbreak peak in T.A.S.
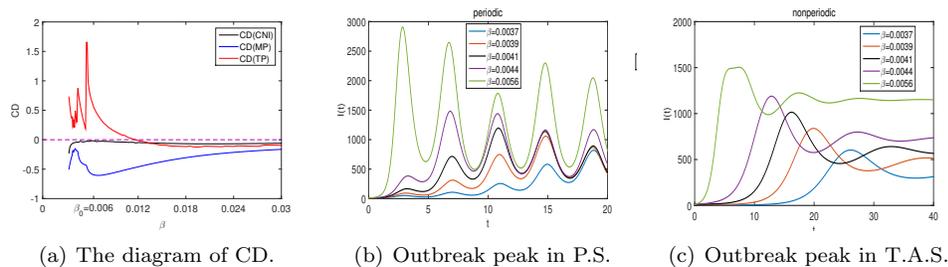
Fig. 6. *Graphs to illustrate the significance of seasonality.*

From Figure 6(a), we observe that the change degree of CNI is relatively small in three quantities after the system (5.1) is averaged to a nonperiodic system that ignores the seasonality in parameters. The underestimation of CNI is about 10%. When $\beta > \beta_0$, the underestimation of MP decreases with the increase of β and TP arrives later and then switches to advance in time. When $\beta < \beta_0$, the underestimation of MP has no monotonicity with respect to β, and CD(TP) fluctuates with respect to β, but TP always arrives later. The reason for these phenomena is as follows. For the nonperiodic system, $I(t)$ has at most two peaks, and the transient highest peak is always the first peak, as shown in Figure 6(c); moreover, the peak value and peak time change continuously as β increases. For the periodic system, $I(t)$ may have several peaks due to seasonality, and the transient highest peak gradually moves from the last peak to the first peak as β increases in Figure 6(b). When $\beta = \beta_0$, the transient highest peak just turns into the first peak. After the transient highest peak becomes the first peak, the peak value and peak time change smoothly. However, before the transient highest peak becomes the first peak, the peak value and peak time vary nonsmoothly. These phenomena indicate that seasonality given in parameters and the infection rate β have complicated effects on disease outbreaks. Therefore, to make an accurate prediction of disease outbreaks, seasonality (or periodicity) of an epidemiological model cannot be ignored.

5.4. Spatio-temporal evolution caused by infection radius and seasonality. In reality, the following question is important in epidemiology: If there is a disease outbreak in a small area of a connected region, when will the rest of the region have a disease outbreak? That is to say, how long is the time difference between these spatially heterogeneous disease outbreaks? We want to explore the spread of diseases' peaks in space over time. In this subsection, we find that with the increase of the infection radius a, the time difference is shortened, and for a very large a, the disease outbreak occurs almost simultaneously in the whole region. We draw the projections of $I(t, x)$ on the $x - t$ plane with the increase of a for the periodic system and the nonperiodic system, respectively; see Figures 7 and 8. In order to observe the evolution of disease in space more clearly, we take a large $l = 300$, and the infected sheep only concentrate in the interval $[149, 151]$ initially. All parameters in the periodic system are the same as those in subsection 5.1, and the parameters in the nonperiodic system are the time averages of the corresponding ones in the periodic system.

For the nonperiodic system, we sketch the spatio-temporal evolution for various infection radii in Figure 7. Figure 7(a) shows that when a = 0 (i.e., local infection), $I(t, x)$ propagates along two yellow regions starting from an interval containing $[149, 151] \subset [0, 300]$ at $t \approx 16$; that is, at about $t = 16$ the number of infected sheep reaches a peak on the interval $[149, 151]$. Over time the peak bifurcates into two peaks, which spread out toward the boundaries, and at $t \approx 35$ the peaks disappear and the infectives diffuse over the whole space. Hence, for the whole region $[0, 300]$, the time from the first peak to the last peak is about 19. Figures 7(b), 7(c), and 7(d) show that $I(t, x)$ has an evolution similar to that of $a = 0$ when $a = 5$, $a = 20$, and $a = 50$. However, we can observe that the time from the first peak to the last peak decreases. When the infection radius a is large enough, the disease outbreak occurs almost simultaneously in the whole region.

The discontinuities in the yellow region of Figure 8 are caused by seasonal factors when system (5.1) is periodic. Similar to the nonperiodic case, with the increase of a, the time from the first peak to the last peak also decreases, and the disease

outbreak occurs almost simultaneously in the whole region. By comparing Figure 8 with Figure 7, we observe that due to seasonality, not all locations experience a major disease outbreak in the early stages of disease transmission when a is relatively small; for example, see Figures 8(a) and 8(b).
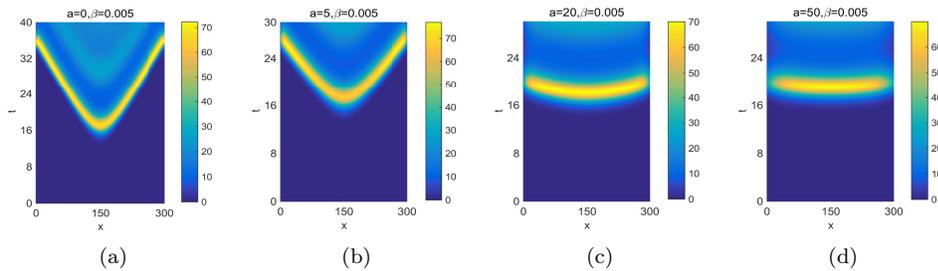
FIG. 7. *Spatio-temporal evolution of $I(t, x)$ with respect to a when* (5.1) *is nonperiodic.*
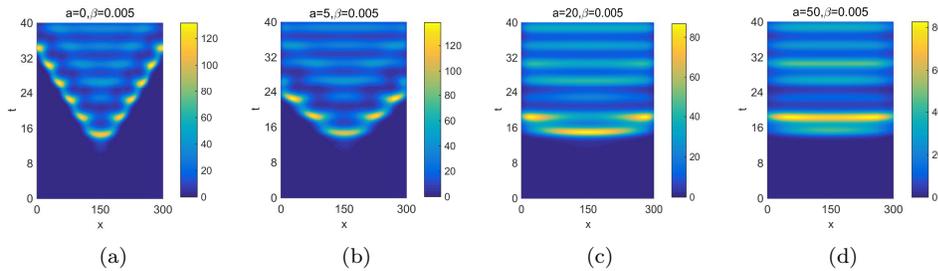
FIG. 8. *Spatio-temporal evolution of $I(t, x)$ with respect to a when* (5.1) *is periodic.*

5.5. Local sensitivity analysis. In this subsection, we analyze the sensitivity indices (S.I.) of two focused quantities to the parameters of (5.1) by computing

$$S.I. = \frac{x^*(1.01p) - x^*(0.99p)}{0.02x^*}$$

as in [17], where x^* is the quantity being considered and p is some parameter that x^* depends on. S.I. can be positive or negative, and a larger absolute value of S.I. indicates that x^* depends more heavily on p. Here x^* is the magnitude of the transient highest outbreak peak (MP) and the time of the transient highest outbreak peak (TP) for $I(t)$, and p is one of the parameters in our model; see Table 1. As discussed in subsection 5.3, the peak value can be larger or smaller and peak time may arrive later or advance in time when a increases; we do not analyze the sensitivity of MP and TP to the parameter a. Note that p can be chosen as a baseline value or a baseline function.

The second column shows the sensitivity indices of MP to each parameter. We can observe that MP has the positive strongest sensitivity to $\Lambda(t)$, and the positivity implies that a higher birth rate would lead to a more severe epidemic. This makes sense because the continuous input of sheep provides more susceptible sheep to be infected. MP is also positively related to β. Increasing the infection rate β will clearly aggravate the disease outbreak. Relatively, the S.I. of MP to $\mu(t)$ and $\nu(t)$

TABLE 1
The sensitivity of MP and TP to the parameters.

Parameter	S.I. of MP	S.I. of TP	Parameter meaning
$\mu(t)$	0.2531	0	diffusion coefficient of susceptibles
$\nu(t)$	0.1256	0	diffusion coefficient of infectives
$d(t)$	-4.4305	0.1066	death rate of susceptibles
$\kappa(t)$	-3.2224	0.1322	death rate of infectives
$\Lambda(t)$	4.9987	-0.1066	birth rate
β	2.2963	-0.1332	infection rate

are very small. This result suggests that although rapid spread of sheep increases the opportunity of contact between susceptible and infected sheep and thereby increases the infection probability, it is not an effective way to control the spread of sheep in mitigating the disease outbreak. The best strategy to relieve the disease outbreak is to decrease the newborns or to reduce the infection rate via methods like isolation and cleansing. MP is negatively related to the death rates $d(t)$ and $\kappa(t)$. This observation implies that slaughtering sheep regardless of whether they are sick or healthy is an effective way to control the disease outbreak, especially when it is difficult to control the newborns and to reduce the infection rate.

The third column shows the sensitivity indices of TP to each parameter. We can observe that TP is far less sensitive to parameters than MP. TP is positively related to the death rates $d(t), \kappa(t)$. TP is negatively related to the birth rate $\Lambda(t)$ and the infection rate β. This makes sense because increasing the number of newborns or the infection rate will result in more sheep being infected and thereby lead to an earlier peak. An additional observation is that TP is irrelevant to the diffusion coefficients $\mu(t)$ and $\nu(t)$.

6. Discussion. In this paper, we theoretically and numerically analyze a diffusive model with seasonality and nonlocal incidence. We not only give the definition of $\mathcal{R}_0$ and the threshold theory but also obtain some new and interesting outcomes about nonlocal incidence and seasonality. Nonlocal incidence describes the situation that susceptibles at a location can be infected by infected individuals at other locations following a probability distribution, whereas local incidence does not take into account the distribution and concentrates the same β on one location. The model with nonlocal incidence leads to the decrease of $\mathcal{R}_0$ by spreading infection probability over space. As Theorem 4.1 shows, if we approximate the nonlocal model to the local model, we will overestimate $\mathcal{R}_0$. Moreover, when the effective infection range becomes larger, $\mathcal{R}_0$ and the endemic size of $I(t)$ both become smaller. However, there is no uniform law for the disease outbreak with respect to the effective infection range. For the nonperiodic system, the transient highest peak of $I(t)$ is the first peak, whereas for the periodic system, due to seasonal factors the transient highest peak of $I(t)$ gradually moves from the back peak to the first peak with the increase of β. The difference leads to different dynamics for the periodic system and the nonperiodic system with the increase of β, especially for the peak value and the peak time of $I(t)$. Note that this complexity is caused by seasonality and β in an integrative way. In addition, because infections occur only at locations of infectives in the absence of nonlocality and infections occur in all neighborhoods of infectives in the presence of nonlocality, diseases spread faster for nonlocal infection, and then individuals quickly achieve group behavior in a short time, that is, collective infection. As shown in subsection 5.4, the time difference between the first peak and the last peak for $I(t, x)$ decreases when the effective infection range becomes larger, and when the effective

infection range is large enough, the disease outbreak occurs almost simultaneously in the whole region. Meanwhile, due to seasonality, not all regions will experience a major disease outbreak in the early stages of disease transmission when the effective infection range is relatively small.

The conclusions of our model (1.3) are also valid for the corresponding autonomous system (1.2) discussed by Orlandi and Tesei in [23]. Compared with [23], we not only give the definition of $\mathcal{R}_0$ and the persistence of solution but also clarify the importance of nonlocal infection. However, the problem of uniqueness and global stability of positive periodic solutions has not been solved. Kuniya and Wang [19] and Thieme [31] both obtained the global asymptotic stability of a positive equilibrium for SIR (PDE) model by constructing Lyapunov functions when at least one of the two diffusion coefficients is zero. In the future, we will investigate how the diffusion coefficient influences positive periodic solutions. In addition, in view of the diversity of transmission mechanisms, we plan to consider a more general periodic nonlocal incidence $\int_\Omega f(t,x,y,S(t,x),I(t,y))dy$ to further the work begun in this paper and [31].

Appendix A. Proof of Theorems 2.1 and 2.2. Let $A_1(t) = \mu(t)\Delta - d(t)id_{C(\overline{\Omega})}$ and $A_2(t) = \nu(t)\Delta - \kappa(t)id_{C(\overline{\Omega})}$ with domain $\mathcal{D}$. Let $\{U_1(t,\tau)\}_{t\geq\tau}$ and $\{U_2(t,\tau)\}_{t\geq\tau}$ be the evolution families on $C(\overline{\Omega})$ generated by $\{A_1(t)\}_{t\in\mathbb{R}}$ and $\{A_2(t)\}_{t\in\mathbb{R}}$, respectively. Then, there are positive constants r_1 and r_2 such that $\|U_1(t,\tau)\| \leq e^{-r_1(t-\tau)}$ and $\|U_2(t,\tau)\| \leq e^{-r_2(t-\tau)}$ for all $t \geq \tau$. We point out that the evolution families $\{U_1(t,\tau)\}_{t\geq\tau}$ and $\{U_2(t,\tau)\}_{t\geq\tau}$ enjoy smoothing effects just like the heat semigroup.

The next result is classical. See [26], for instance.

LEMMA A.1 (local well-posedness and positivity). *For any $(S_\tau, I_\tau) \in X$, there exists a maximal $T_{\max} > \tau$ such that (1.3) admits a unique classical solution $(S, I) \in C([\tau, T_{\max}), X) \cap C^1((\tau, T_{\max}), \mathcal{D} \times \mathcal{D})$ with initial data (S_τ, I_τ) at initial moment τ. Moreover, the following statements hold.*

(1) *If $T_{\max} < \infty$, then $\lim_{t \to T_{\max}^-} \|(S(t), I(t))\|_X = \infty$.*
(2) *If $(S_\tau, I_\tau) \in X_+$, then $(S(t), I(t)) \in X_+$ for all $t \in (\tau, T_{\max})$.*
(3) *If $(S_\tau, I_\tau) \in X_+$ and $I_\tau \not\equiv 0$, then $(S(t), I(t)) \in X_{++}$ for all $t \in (\tau, T_{\max})$.*

We first prove Theorem 2.1.

Proof of Theorem 2.1. Let $(S(t), I(t))$ be the unique solution of (1.3) with initial data (S_τ, I_τ) at the initial moment τ on the maximal interval of existence $[\tau, T_{\max})$. Given Lemma A.1, it suffices to show that $\sup_{t\in[\tau,T_{\max})} \|(S(t), I(t))\|_X < \infty$.

Assume without loss that $\tau = 0$. Since β, K, S, and I are nonnegative, we find from the variation of constants formula that $S(t) \leq U_1(t,0)S_0 + \int_0^t U_1(t,s)\Lambda(s)ds$ for all $t \in [0, T_{\max})$. This leads to

$$(A.1) \qquad \|S(t)\|_\infty \leq e^{-r_1 t}\|S_0\|_\infty + \frac{\Lambda_{\max}}{r_1}\left(1 - e^{-r_1 t}\right), \quad t \in [0, T_{\max}),$$

where $\Lambda_{\max} = \max_{t\in[0,T]} \Lambda(t)$. It follows that

$$(A.2) \qquad \sup_{t\in[0,T_{\max})} \|S(t)\|_\infty \leq \|S_0\|_\infty + \frac{\Lambda_{\max}}{r_1}.$$

It remains to show that $\sup_{t\in[0,T_{\max})} \|I(t)\|_\infty < \infty$. Clearly, for $t \in (0, T_{\max})$,

$$\frac{d}{dt}\left[\int_\Omega S(t,x)dx + \int_\Omega I(t,x)dx\right] \leq \Lambda_{\max}|\Omega| - \gamma\left[\int_\Omega S(t,x)dx + \int_\Omega I(t,x)dx\right],$$

where $|\Omega|$ is the Lebesgue measure of Ω and $\gamma = \inf_{t\in[0,T]} \min\{d(t), \kappa(t)\}$. It follows in particular that

$$(A.3) \qquad \int_\Omega I(t,x)dx \le e^{-\gamma t}|\Omega| \left(\|S_0\|_\infty + \|I_0\|_\infty\right) + \frac{\Lambda_{\max}|\Omega|}{\gamma}, \quad t \in [0, T_{\max}).$$

We find from the variation of constants formula that

$$\|I(t)\|_\infty \le e^{-r_2 t}\|I_0\|_\infty + \beta \int_0^t e^{-r_2(t-s)} \left\|S(s,\cdot)\int_\Omega K(s,\cdot - y)I(s,y)dy\right\|_\infty ds$$

$$\le e^{-r_2 t}\|I_0\|_\infty + C_1 \int_0^t e^{-r_2(t-s)} \left[\int_\Omega I(s,y)dy\right] ds, \quad t \in [0, T_{\max}),$$

where we used (A.2) and $C_1 := \beta(\|S_0\|_\infty + \frac{\Lambda_{\max}}{r_1})\sup_{(t,x,y)\in\mathbb{R}_+\times\overline{\Omega}\times\overline{\Omega}} K(t, x-y)$. Replacing γ by a smaller number such that $\gamma < r_2$, we find from (A.3) that

$$\|I(t)\|_\infty \le e^{-r_2 t}\|I_0\|_\infty + C_1 \int_0^t e^{-r_2(t-s)} \left[e^{-\gamma s}|\Omega|\left(\|S_0\|_\infty + \|I_0\|_\infty\right) + \frac{\Lambda_{\max}|\Omega|}{\gamma}\right] ds$$

$$\le e^{-r_2 t}\|I_0\|_\infty + C_1|\Omega|\left(\|S_0\|_\infty + \|I_0\|_\infty\right)\frac{1}{r_2-\gamma}e^{-\gamma t}\left(1 - e^{-(r_2-\gamma)t}\right)$$

$$+ C_1\frac{\Lambda_{\max}|\Omega|}{\gamma}\frac{1}{r_2}\left(1 - e^{-r_2 t}\right), \quad t \in [0, T_{\max}).$$

This completes the proof. □

Now, we prove Theorem 2.2.

Proof of Theorem 2.2. By the regularity theory of parabolic equations, the map $\mathcal{P}$ is compact. For the existence of a global attractor, we need to show that $\mathcal{P}$ admits a bounded absorbing set, namely, a bounded set $B_* \subset X_+$ such that for any bounded set $B \subset X_+$ there is an integer $n_0 = n_0(B) > 0$ such that $\mathcal{P}^n B \subset B_*$ for all $n \ge n_0$.

Let $B \subset X_+$ be bounded. For $(S_0, I_0) \in B$, let $(S(t;u_0), I(t;u_0)) = \Sigma(t,0)(S_0, I_0)$ be the unique solution of (1.3) given in Theorem 2.1. By (A.1), there is $t_1 = t_1(B) > 0$ such that $\{S(t;u_0) : u_0 \in B\} \subset B_*^1 := \{S \in C(\overline{\Omega}) : \|S\|_\infty \le 1 + \frac{\Lambda_{\max}}{r_1}\}$ for all $t \ge t_1$.

By (A.3), we find $t_2 = t_2(B) \ge t_1(B)$ such that $\sup_{u_0\in B}\int_\Omega I(t,x;u_0)dx \le 1 + \frac{\Lambda_{\max}|\Omega|}{\gamma}$ for all $t \ge t_2$. It follows from the variation of constants formula that

$$\|I(t;u_0)\|_\infty \le e^{-r_2(t-t_2)}\|I_0(t_2;u_0)\|_\infty + C_2 \int_{t_2}^t e^{-r_2(t-s)}\left[\int_\Omega I(s,y;u_0)dy\right] ds$$

$$\le e^{-r_2(t-t_2)}\|I_0(t_2;u_0)\|_\infty + C_3, \quad t \in [t_2, \infty),$$

where $C_2 := \beta(1 + \frac{\Lambda_{\max}}{r_1})\sup_{(t,x,y)\in\mathbb{R}_+\times\overline{\Omega}\times\overline{\Omega}} K(t, x-y)$ and $C_3 := \frac{C_2}{r_2}(1 + \frac{\Lambda_{\max}|\Omega|}{\gamma})$.

Since $\sup_{u_0\in B}\|I_0(t_2;u_0)\|_\infty < \infty$ with the upper bound depending only on B, we find $t_3 = t_3(B) \ge t_2$ such that $\{I(t;u_0) : u_0 \in B\} \subset B_*^2$ for all $t \ge t_3$, where $B_*^2 := \{I \in C(\overline{\Omega}) : \|I\|_\infty \le 1 + C_3\}$.

Set $B_* = B_*^1 \times B_*^2$, which is universal. Letting $n_0 = n_0(B) \ge t_3$, we find $\mathcal{P}^n B = \Sigma(n,0)B \subset B_*$ for all $n \ge n_0$. This completes the proof. □

Appendix B. Proof of Theorem 3.1. We follow [27, Theorem 3.3] and [38, Theorem 13.2.1] to prove Theorem 3.1. Before proving Theorem 3.1, we derive some properties of the map $\mathcal{P}$. Let

$$X_+^0 := \{(S, I) \in X_+ : I \not\equiv 0\} \quad \text{and} \quad \partial X_+^0 := X_+ \setminus X_+^0 = \{(S, I) \in X_+ : I \equiv 0\}.$$

Clearly, $\mathcal{P}X_+^0 \subset X_+^0$ and $\mathcal{P}\partial X_+^0 \subset \partial X_+^0$.

DEFINITION B.1. *The map $\mathcal{P}$ is said to be* uniformly persistent *with respect to $(X_+^0, \partial X_+^0)$ if there exists $\epsilon_0 > 0$ such that $\liminf_{n\to\infty} d_{X_+}(\mathcal{P}^n u, \partial X_+^0) \geq \epsilon_0$ for any $u \in X_+^0$, where the distance d_{X_+} is generated by the norm on X_+.*

LEMMA B.1. *If $\mathcal{R}_0 > 1$, then $\mathcal{P}$ is uniformly persistent with respect to $(X_+^0, \partial X_+^0)$.*

Proof. We first study the dynamics of $\mathcal{P}$ on ∂X_+^0. Note that if $(S_0, I_0) \in \partial X_+^0$, then $I(t, \cdot) \equiv 0$ for all $t > 0$. As a result, $S(t, x)$ satisfies $S_t = \mu(t)\Delta S + \Lambda(t) - d(t)S$ with homogeneous Neumann boundary condition on $\partial\Omega$. By spectral analysis and the comparison principle, it is not hard to see that $\|S(t) - S^0(t)\|_\infty \to 0$ as $t \to \infty$. As a result, for any $(S_0, I_0) \in \partial X_+^0$, there holds

(B.1) $$\left\|\mathcal{P}^n(S_0, I_0) - \left(S^0(0), 0\right)\right\|_X \to 0 \quad \text{as} \quad n \to \infty.$$

Next, let $W^s := \left\{u \in X_+ : \mathcal{P}^n u \to \left(S^0(0), 0\right) \text{ in } X_+ \text{ as } n \to \infty\right\}$ be the stable manifold of $\left(S^0(0), 0\right)$ in X_+. We show that

(B.2) $$W^s \cap X_+^0 = \emptyset.$$

This is clearly the case if we can show that

(B.3) $$\exists \delta > 0 \text{ s.t. } \limsup_{n\to\infty} \left\|\mathcal{P}^n u - \left(S^0(0), 0\right)\right\|_X \geq \delta \quad \forall u \in X_+^0.$$

Note that (B.3) is equivalent to the following claim:

(B.4) $$\forall 0 < \delta \ll 1, \text{ there holds } \limsup_{n\to\infty} \left\|\mathcal{P}^n u - \left(S^0(0), 0\right)\right\|_X \geq \delta \quad \forall u \in X_+^0.$$

Indeed, it is obvious to see that (B.4) is stronger than (B.3). Conversely, if (B.3) holds with $\delta = \delta_*$ for some $\delta_* > 0$, then for any $\delta \in (0, \delta_*]$ there holds

$$\limsup_{n\to\infty} \left\|\mathcal{P}^n u - \left(S^0(0), 0\right)\right\|_X \geq \delta_* \geq \delta \quad \forall u \in X_+^0.$$

This in particular implies (B.4). Hence, (B.3) and (B.4) are equivalent.

We prove (B.4). Suppose it fails. Then, there is a sufficiently small $\delta_0 > 0$ and a corresponding initial data $(S_0^*, I_0^*) \in X_{++}$ such that

(B.5) $$\left\|\mathcal{P}^n(S_0^*, I_0^*) - \left(S^0(0), 0\right)\right\|_X \leq \delta_0 \quad \forall n \geq 0.$$

Denote by $(S^*(t), I^*(t)) = (S^*(t, \cdot), I^*(t, \cdot))$ the unique solution of (1.3) with initial data (S_0^*, I_0^*). For $t > 0$, let $[t]$ be the largest integer satisfying $[t]T \leq t$, and set $r_t = t - [t]T \in [0, T)$. Then, $(S^*(t), I^*(t)) = \Sigma(r_t, 0)\mathcal{P}^{[t]}(S_0^*, I_0^*)$. Due to the continuous dependence of solutions of (1.3) on the initial data and (B.5), there is a continuous function $\eta : \mathbb{R}_+ \to \mathbb{R}_+$ satisfying $\eta(0) = 0$ and $\eta(\delta) \to 0$ as $\delta \to 0^+$ such that $\left\|(S^*(t), I^*(t)) - \left(S^0(t), 0\right)\right\|_X \leq \eta(\delta_0)$ for all $t \geq 0$.

Setting $\epsilon_0 = \eta(\delta_0)$, we find that $I^*(t, x)$ satisfies

$$\begin{cases} I_t^* \geq \nu(t)\Delta I^* - \kappa(t)I^* + \beta\left[S^0(t) - \epsilon_0\right] \int_\Omega K(t, x-y)I^*(t, y)dy, & x \in \Omega, \\ \mathbf{n}(x) \cdot \nabla I^*(t, x) = 0, & x \in \partial\Omega, \end{cases}$$

for $t > 0$. Consider the operator $\mathcal{L}^0 : \mathcal{D}_T(\mathbb{R} \times \overline{\Omega}) \to C_T(\mathbb{R} \times \overline{\Omega})$ defined by

$$\mathcal{L}^0[\phi](t, x) = -\phi_t(t, x) + \nu(t)\Delta\phi(t, x) - \kappa(t)\phi(t, x)$$
$$+ \beta\left[S^0(t) - \epsilon_0\right] \int_\Omega K(t, x-y)\phi(t, y)dy, \quad (t, x) \in \mathbb{R} \times \overline{\Omega},$$

for $\phi \in \mathcal{D}_T(\mathbb{R} \times \overline{\Omega})$. Lemma 3.2 holds with $\mathcal{L}$ replaced by $\mathcal{L}^0$. Moreover, by the continuous dependence of the principal eigenvalue on parameters, we find that the principal eigenvalue λ_p^0 of $\mathcal{L}^0$ is positive as $\lambda_p > 0$, which is equivalent to $\mathcal{R}_0 > 1$.

Let ϕ^0 be a principal eigenfunction of $\mathcal{L}^0$ associated to λ_p^0. Since $I^* \in C_{++}(\overline{\Omega})$, there is a $c^* > 0$ such that $I^* \geq c^* \phi^0(0, \cdot)$ on $\overline{\Omega}$. As $e^{\lambda_p^0 t} c^* \phi^0(t, x)$ solves the equation

$$\begin{cases} J_t = \nu(t)\Delta J - \kappa(t)J + \beta\left[S^0(t) - \epsilon_0\right] \int_\Omega K(t, x - y)J(t, y)dy, & x \in \Omega, \\ \mathbf{n}(x) \cdot \nabla J(t, x) = 0, & x \in \partial\Omega, \end{cases}$$

for $t > 0$, we conclude from the comparison principle that $I^*(t, x) \geq e^{\lambda_p^0 t} c^* \phi^0(t, x)$ for $x \in \overline{\Omega}$ and $t > 0$. The time-periodicity of ϕ^0 and the positivity of λ_p^0 then yield $\min_{x \in \overline{\Omega}} I^*(t, x) \to \infty$ as $t \to \infty$, which leads to a contradiction. This proves (B.4).

In the presence of (B.1) and (B.2), we can apply well-known results on uniform persistence (see, e.g., [37, Theorem 2.2]) to conclude that $\mathcal{P}$ is uniformly persistent with respect to $(X_+^0, \partial X_+^0)$. $\square$

Now, we prove Theorem 3.1.

Proof of Theorem 3.1. (1) Clearly, $S(t, x)$ satisfies $S_t \leq \mu(t)\Delta S + \Lambda(t) - d(t)S$ on $(0, \infty) \times \Omega$ with homogeneous Neumann boundary condition on $\partial\Omega$. By the comparison principle, for any $\epsilon > 0$, there is $t_\epsilon > 0$, depending on the initial data, such that

(B.6) $$\|S(t)\|_\infty \leq S^0(t) + \epsilon, \quad t \geq t_\epsilon.$$

Fix a sufficiently small ϵ. we see that $I(t, x)$ satisfies

$$\begin{cases} I_t \leq \nu(t)\Delta I - \kappa(t)I + \beta\left[S^0(t) + \epsilon\right] \int_\Omega K(t, x - y)I(t, y)dy, & x \in \Omega, \quad t > t_\epsilon, \\ \mathbf{n}(x) \cdot \nabla I(t, x) = 0, & x \in \partial\Omega, \quad t > t_\epsilon. \end{cases}$$

Consider the operator $\mathcal{L}^\epsilon : \mathcal{D}_T(\mathbb{R} \times \overline{\Omega}) \to C_T(\mathbb{R} \times \overline{\Omega})$ defined by

$$\mathcal{L}^\epsilon[\phi](t, x) = -\phi_t(t, x) + \nu(t)\Delta\phi(t, x) - \kappa(t)\phi(t, x)$$
$$+ \beta\left[S^0(t) + \epsilon\right] \int_\Omega K(t, x - y)\phi(t, y)dy, \quad (t, x) \in \mathbb{R} \times \overline{\Omega},$$

for $\phi \in \mathcal{D}_T(\mathbb{R} \times \overline{\Omega})$. Lemma 3.2 holds with $\mathcal{L}$ replaced by $\mathcal{L}^\epsilon$. Moreover, by the continuous dependence of the principal eigenvalue on parameters, we find that the principal eigenvalue λ_p^ϵ of $\mathcal{L}^\epsilon$ is negative as $\lambda_p < 0$, which is equivalent to $\mathcal{R}_0 < 1$.

Let ϕ^ϵ be a principal eigenfunction of $\mathcal{L}^\epsilon$ associated to λ_p^ϵ. Clearly, there is a $c^\epsilon > 0$ such that $I(t_\epsilon) \leq c^\epsilon \phi^\epsilon(t_\epsilon, \cdot)$ on $\overline{\Omega}$. As $e^{\lambda_p^\epsilon(t - t_\epsilon)} c^\epsilon \phi^\epsilon(t, x)$ solves the equation

$$\begin{cases} J_t = \nu(t)\Delta J - \kappa(t)J + \beta\left[S^0(t) - \epsilon\right] \int_\Omega K(t, x - y)J(t, y)dy, & x \in \Omega, \quad t > t_\epsilon, \\ \mathbf{n}(x) \cdot \nabla J(t, x) = 0, & x \in \partial\Omega, \quad t > t_\epsilon, \end{cases}$$

we conclude from the comparison principle that

(B.7) $$I(t, x) \leq e^{\lambda_p^\epsilon(t - t_\epsilon)} c^\epsilon \phi^\epsilon(t, x), \quad x \in \overline{\Omega}, \quad t > t_\epsilon.$$

This implies that $\|I(t)\|_\infty \to 0$ as $t \to \infty$.

Let $C_\epsilon := \beta \sup_{(t, x, y) \in [t_\epsilon, \infty) \times \overline{\Omega} \times \overline{\Omega}} \{[S^0(t) + \epsilon] K(t, x - y) e^{-\lambda_p^\epsilon t_\epsilon} c^\epsilon \phi^\epsilon(t, y)\}$. We see from (B.7) that

$$\begin{cases} S_t \geq \mu(t)\Delta S + \Lambda(t) - d(t)S - C_\epsilon|\Omega|e^{\lambda_p^\epsilon t}, & x \in \Omega, \quad t > t_\epsilon, \\ \mathbf{n}(x) \cdot \nabla S(t, x) = 0, & x \in \partial\Omega, \quad t > t_\epsilon. \end{cases}$$

Let us consider the solution of the ODE $\dot{h} = \Lambda(t) - d(t)h - C_\epsilon|\Omega|e^{\lambda_p^\epsilon t}$ for $t > t_\epsilon$ with initial condition $h(t_\epsilon) = \min_{x \in \overline{\Omega}} S(t_\epsilon, x)$. Using the variation of constants formula, it is not hard to see that $|h(t) - S^0(t)| \to 0$ as $t \to \infty$. By the comparison principle, we find $S(t, x) \geq h(t)$ for $x \in \overline{\Omega}$ and $t \geq t_\epsilon$. Hence, $\liminf_{t \to \infty} \left[\min_{x \in \overline{\Omega}} S(t, x) - S^0(t) \right] \geq 0$. This together with (B.6) leads to $\|S(t, \cdot) - S^0(t)\|_{C(\overline{\Omega})} \to 0$ as $t \to \infty$.

(2) By the compactness of $\mathcal{P}$, Theorem 2.2, and Lemma B.1, we apply [37, Theorem 2.3] to conclude that $\mathcal{P}$ has a fixed point in X_+^0 and, restricting to X_+^0, admits a global attractor $\mathcal{A}^0$ attracting strongly bounded sets in X_+^0, namely, bounded sets in X_+^0 staying away from ∂X_+^0. As $\mathcal{A}^0 = \mathcal{P}\mathcal{A}^0$, there holds $\mathcal{A}^0 \subset X_{++}$, which implies that $\cup_{t \in [0,T]} \Sigma(t, 0)\mathcal{A}^0 \subset X_{++}$. As the fixed point of $\mathcal{P}$ must lie in $\mathcal{A}^0$, it gives a T-periodic solution of (1.3) in X_{++}.

Now, for any $(S_0, I_0) \in X_+^0$ with $I_0 \not\equiv 0$, we find $\lim_{n \to \infty} d_H(\mathcal{P}^n(S_0, I_0), \mathcal{A}^0) = 0$, which implies that $d_H((S(t), I(t)), \Sigma(t, 0)\mathcal{A}^0) \to 0$ as $t \to \infty$. Since $\Sigma(t, 0)\mathcal{A}^0 \subset \cup_{t \in [0,T]} \Sigma(t, 0)\mathcal{A}^0 \subset X_{++}$ for all $t \geq 0$, there exists some $\epsilon_0 > 0$, depending only on $\cup_{t \in [0,T]} \Sigma(t, 0)\mathcal{A}^0$, such that $\liminf_{t \to \infty} \min_{x \in \overline{\Omega}} \min\{S(t, x), I(t, x)\} \geq \epsilon_0$. This completes the proof. $\square$

Appendix C. Proof of Theorem 4.1.

Proof of Theorem 4.1. (1) Note that we can consider $\mathcal{N}^a$ and $\mathcal{N}^0$ as operators on $C_T(\mathbb{R}; L^2(\Omega))$, the space of all $L^2(\Omega)$-valued continuous and periodic functions on $\mathbb{R}$. By parabolic regularity or the smoothing effect of the evolution family $\{U_2(t, s)\}_{t \geq s}$, $\mathcal{R}_0^a$ and $\mathcal{R}_0^0$ are still the spectral radii, and algebraically simple and isolated eigenvalues of $\mathcal{N}^a$ and $\mathcal{N}^0$, respectively. Since for each $\phi \in C_T(\mathbb{R}; L^2(\Omega))$, $\int_\Omega K_a(t, \cdot - y)\phi(t, y)dy$ converges in $L^2(\Omega)$ to $\phi(t, \cdot)$ uniformly in $t \in \mathbb{R}$ as $a \to 0^+$, we conclude from the compactness of $U_2(t, s)$ for $t > s$ that $\mathcal{N}^a$ converges in norm to $\mathcal{N}^0$ as $a \to 0^+$. It then follows from the well-known result on the continuity of isolated eigenvalues under perturbations (see, e.g., [12, Chapter IV, section 3.5]) that $\lim_{a \to 0^+} \mathcal{R}_0^a = \mathcal{R}_0^0$.

(2) Note that $S^0(t) = S^0$ is independent of t. Let us recall Lemma 3.3(1) and point out that a similar result holds for $\mathcal{N}^0$ or $\mathcal{R}_0^0$. For $a > 0$, let $\phi^a \in \mathcal{D}_T(\mathbb{R} \times \overline{\Omega})$ be positive and satisfy

(C.1)
$$
\begin{cases}
\phi_t^a = \nu(t)\Delta\phi^a - \kappa\phi^a + \frac{\beta S^0}{\mathcal{R}_0^a} \int_\Omega K_a(t, x-y)\phi^a(t, y)dy, & (t, x) \in \mathbb{R} \times \Omega, \\
\mathbf{n}(x) \cdot \nabla\phi^a(t, x) = 0, & (t, x) \in \mathbb{R} \times \partial\Omega,
\end{cases}
$$

and let $\phi^0 \in \mathcal{D}_T(\mathbb{R} \times \overline{\Omega})$ be positive and satisfy the equation $\phi_t^0 = \nu(t)\Delta\phi^0 - \kappa\phi^0 + \frac{\beta S^0}{\mathcal{R}_0^0}\phi^0$ on $\mathbb{R} \times \Omega$ with homogeneous Neumann boundary condition on $\mathbb{R} \times \partial\Omega$. It is easy to see that ϕ^0 must be a constant function and $\mathcal{R}_0^0 = \frac{\beta S^0}{\kappa}$.

Multiplying (C.1) by ϕ^a and integrating the resulting equation over $[0, T] \times \Omega$ lead to
$$
\mathcal{R}_0^a = \frac{\beta S^0 \int_0^T \int_\Omega \int_\Omega K_a(t, x-y)\phi^a(t, y)\phi^a(t, x)dxdydt}{\int_0^T \nu(t)\|\nabla\phi^a(t, \cdot)\|_{L^2}^2 dt + \kappa \int_0^T \|\phi^a(t, \cdot)\|_{L^2}^2 dt}.
$$

We see that
$$
\int_\Omega \int_\Omega K_a(t, x-y)\phi^a(t, y)\phi^a(t, x)dxdy
$$
$$
\leq \left[\int_\Omega \int_\Omega K_a(t, x-y)(\phi^a(t, y))^2 dxdy \right]^{\frac{1}{2}} \left[\int_\Omega \int_\Omega K_a(t, x-y)(\phi^a(t, x))^2 dxdy \right]^{\frac{1}{2}}
$$
$$
< \|\phi^a(t, \cdot)\|_{L^2}^2,
$$

where we used the facts that $\int_\Omega K_a(t, x - \cdot)dx \lesseqgtr 1$ and $\int_\Omega K_a(\cdot - y)dy \lesseqgtr 1$ in the last inequality, from which we deduce that $\mathcal{R}_0^a < \frac{\beta S^0}{\kappa} = \mathcal{R}_0^0$ for $a > 0$. $\qquad\square$

REFERENCES

[1] R. M. ANDERSON AND R. M. MAY, *Infectious Diseases of Humans: Dynamics and Control*, Oxford University Press, Oxford, UK, 1991.

[2] L. J. S. ALLEN, B. M. BOLKER, Y. LOU, AND A. L. NEVAI, *Asymptotic profiles of the steady states for an SIS epidemic reaction-diffusion model*, Discrete Contin. Dyn. Syst., 21 (2008), pp. 1–20, https://doi.org/10.3934/dcds.2008.21.1.

[3] N. BACAËR AND S. GUERNAOUI, *The epidemic threshold of vector-borne diseases with seasonality: The case of cutaneous leishmaniasis in Chichaoua, Morocco*, J. Math. Biol., 53 (2006), pp. 421–436, https://doi.org/10.1007/s00285-006-0015-0.

[4] N. T. J. BAILEY, *The Mathematical Theory of Infectious Diseases and Its Applications*, 2nd ed., Hafner Press, Macmillan, New York, 1975.

[5] E. A. BAUMGARTNER, N. C. DAO, S. NASREEN, M. U. BHUIYAN, S. MAH-E-MUNEER, ET AL., *Seasonality, timing, and climate drivers of influenza activity worldwide*, J Infect. Dis., 206 (2012), pp. 838–846, https://doi.org/10.1093/infdis/jis467.

[6] H. GUO, M. Y. LI, AND Z. SHUAI, *A graph-theoretic approach to the method of global Lyapunov functions*, Proc. Amer. Math. Soc., 136 (2008), pp. 2793–2802, https://doi.org/10.1090/S0002-9939-08-09341-6.

[7] P. HESS, *Periodic-Parabolic Boundary Value Problems and Positivity*, Pitman Res. Notes Math. 247, Longman, Harlow, UK, John Wiley & Sons, New York, 1991.

[8] H. W. HETHCOTE, *Qualitative analyses of communicable disease models*, Math. Biosci., 28 (1976), pp. 335–356, https://doi.org/10.1016/0025-5564(76)90132-2.

[9] H. W. HETHCOTE, *The mathematics of infectious diseases*, SIAM Rev., 42 (2000), pp. 599–653, https://doi.org/10.1137/S0036144500371907.

[10] W. Z. HUANG, M. HAN, AND K. LIN, *Dynamics of an SIS reaction-diffusion epidemic model for disease transmission*, Math. Biosci. Eng., 7 (2010), pp. 51–66, https://doi.org/10.3934/mbe.2010.7.51.

[11] H. INABA, *On a new perspective of the basic reproduction number in heterogeneous environments*, J. Math. Biol., 65 (2012), pp. 309–348, https://doi.org/10.1007/s00285-011-0463-z.

[12] T. KATO, *Perturbation Theory for Linear Operators*, reprint of the 1980 edition, Classics in Math., Springer-Verlag, Berlin, 1995.

[13] W. KERMACK AND A. MCKENDRICK, *A contribution to the mathematical theory of epidemics*, Proc. Roy. Soc. Lond. A, 115 (1927), pp. 700–721, https://doi.org/10.1098/rspa.1927.0118.

[14] W. KERMACK AND A. MCKENDRICK, *Contributions to the mathematical theory of epidemics—I*, Bull. Math. Biol., 53 (1991), pp. 33–55, https://doi.org/10.1016/S0092-8240(05)80040-0.

[15] W. KERMACK AND A. MCKENDRICK, *Contributions to the mathematical theory of epidemics—II: The problem of endemicity*, Bull. Math. Biol., 53 (1991), pp. 57–87, https://doi.org/10.1016/S0092-8240(05)80041-2.

[16] W. KERMACK AND A. MCKENDRICK, *Contributions to the mathematical theory of epidemics—III: Further studies of the problem of endemicity*, Bull. Math. Biol., 53 (1991), pp. 89–118, https://doi.org/10.1016/S0092-8240(05)80042-4.

[17] J. D. KONG, W. DAVIS, X. LI, AND H. WANG, *Stability and sensitivity analysis of the iSIR model for indirectly transmitted infectious diseases with immunological threshold*, SIAM J. Appl. Math., 74 (2014), pp. 1418–1441, https://doi.org/10.1137/140959638.

[18] M. G. KREĬN AND M. A. RUTMAN, *Linear operators leaving invariant a cone in a Banach space*, Uspehi Matem. Nauk (N. S.), 3 (1948), pp. 3–95 (in Russian).

[19] T. KUNIYA AND J. WANG, *Lyapunov functions and global stability for a spatially diffusive SIR epidemic model*, Appl. Anal., 96 (2017), pp. 1935–1960, https://doi.org/10.1080/00036811.2016.1199796.

[20] X. LIANG, L. ZHANG, AND X.-Q. ZHAO, *Basic reproduction ratios for periodic abstract functional differential equations (with application to a spatial model for Lyme disease)*, J. Dynam. Differential Equations, 31 (2019), pp. 1247–1278, https://doi.org/10.1007/s10884-017-9601-7.

[21] Y. Lou and X.-Q. Zhao, *Threshold dynamics in a time-delayed periodic SIS epidemic model*, Discrete Contin. Dyn. Syst. Ser. B, 12 (2009), pp. 169–186, https://doi.org/10.3934/dcdsb.2009.12.169.

[22] M. Y. Li and Z. Shuai, *Global-stability problem for coupled systems of differential equations on networks*, J. Differential Equations, 248 (2010), pp. 1–20, https://doi.org/10.1016/j.jde.2009.09.003.

[23] P. de Mottoni, E. Orlandi, and A. Tesei, *Asymptotic behavior for a system describing epidemics with migration and spatial spread of infection*, Nonlinear Anal., 3 (1979), pp. 663–675, https://doi.org/10.1016/0362-546X(79)90095-6.

[24] M. Marteheva, *An Introduction to Mathematical Epidemiology*, Texts Appl. Math. 61, Springer, New York, 2015.

[25] E. W. Ng and M. Geller, *A table of integrals of the error functions*, J. Res. Nat. Bur. Standards Sect. B, 73B (1969), pp. 1–20.

[26] A. Pazy, *Semigroups of Linear Operators and Applications to Partial Differential Equations*, Appl. Math. Sci. 44, Springer-Verlag, New York, 1983.

[27] R. Peng and X.-Q. Zhao, *A reaction-diffusion SIS epidemic model in a time-periodic environment*, Nonlinearity, 25 (2012), pp. 1451–1471, https://doi.org/10.1088/0951-7715/25/5/1451.

[28] J. Pizarro-Cerdá, S. Méresse, R. G. Parton, et al., *Brucella abortus transits through the autophagic pathway and replicates in the endoplasmic reticulum of nonprofessional phagocytes*, Infect. Immun., 66 (1998), pp. 5711–5724.

[29] J. Shaman, E. Goldstein, and M. Lipsitch, *Absolute humidity and pandemic versus epidemic influenza*, Amer. J Epidemiol., 173 (2011), pp. 127–235, https://doi.org/10.1093/aje/kwq347.

[30] P. Takáč, *A short elementary proof of the Kreĭn-Rutman theorem*, Houston J. Math., 20 (1994), pp. 93–98.

[31] H. R. Thieme, *Global stability of the endemic equilibrium in infinite dimension: Lyapunov functions and positive operators*, J. Differential Equations, 250 (2011), pp. 3772–3801, https://doi.org/10.1016/j.jde.2011.01.007.

[32] W. Wang and X.-Q. Zhao, *Threshold dynamics for compartmental epidemic models in periodic environments*, J. Dynam. Differential Equations, 20 (2008), pp. 699–717, https://doi.org/10.1007/s10884-008-9111-8.

[33] G. F. Webb, *A reaction-diffusion model for a deterministic diffusive epidemic*, J. Math. Anal. Appl., 84 (1981), pp. 150–161, https://doi.org/10.1016/0022-247X(81)90156-6.

[34] Y. Wu and X. Zou, *Asymptotic profiles of steady states for a diffusive SIS epidemic model with mass action infection mechanism*, J. Differential Equations, 261 (2016), pp. 4424–4447, https://doi.org/10.1016/j.jde.2016.06.028.

[35] L. Zhang, Z.-C. Wang, and X.-Q. Zhao, *Threshold dynamics of a time periodic reaction-diffusion epidemic model with latent period*, J. Differential Equations, 258 (2015), pp. 3011–3036, https://doi.org/10.1016/j.jde.2014.12.032.

[36] Y. Zhang and X.-Q. Zhao, *A reaction-diffusion Lyme disease model with seasonality*, SIAM J. Appl. Math., 73 (2013), pp. 2077–2099, https://doi.org/10.1137/120875454.

[37] X.-Q. Zhao, *Uniform persistence and periodic coexistence states in infinite-dimensional periodic semiflows with applications*, Canad. Appl. Math. Quart., 3 (1995), pp. 473–495.

[38] X.-Q. Zhao, *Dynamical Systems in Population Biology*, 2nd ed., CMS Books Math./Ouvrages Math. SMC, Springer, Cham, 2017.